

# Evolved stars and the origin of abundance trends in planet hosts

★,★★

J. Maldonado<sup>1</sup> and E. Villaver<sup>2</sup>

<sup>1</sup> INAF - Osservatorio Astronomico di Palermo, Piazza Parlamento 1, I-90134 Palermo, Italy

<sup>2</sup> Universidad Autónoma de Madrid, Dpto. Física Teórica, Módulo 15, Facultad de Ciencias, Campus de Cantoblanco, 28049 Madrid, Spain

Received ; accepted

## ABSTRACT

**Context.** Detailed chemical abundance studies have revealed different trends between samples of planet and non-planet hosts. Whether these trends are related to the presence of planets or not is strongly debated. At the same time, tentative evidence that the properties of evolved stars with planets may be different from what we know for main-sequence hosts has been recently reported.

**Aims.** We aim to test whether evolved stars with planets show any chemical peculiarity that could be related to the planet formation process.

**Methods.** We determine in a consistent way the metallicity and individual abundances of a large sample of evolved (subgiants and red giants) and main-sequence stars with and without known planetary companions, and discuss their metallicity distribution and trends. Our methodology is based on the analysis of high-resolution échelle spectra ( $R \gtrsim 57\,000$ ) from 2-3 m class telescopes. It includes the calculation of the fundamental stellar parameters, as well as, individual abundances of C, O, Na, Mg, Al, Si, S, Ca, Sc, Ti, V, Cr, Mn, Co, Ni, and Zn.

**Results.** No differences in the  $\langle [X/Fe] \rangle$  vs. condensation temperature ( $T_C$ ) slopes are found between the samples of planet and non-planet hosts when all elements are considered. However, if the analysis is restricted to only refractory elements, differences in the  $T_C$ -slopes between stars with and without known planets are found. This result is found to be dependent on the stellar evolutionary stage, as it holds for main-sequence and subgiant stars, while there seem to be no difference between planet and non-planet hosts among the sample of giants. A search for correlations between the  $T_C$ -slope and the stellar properties reveals significant correlations with the stellar mass and the stellar age. The data also suggest that differences in terms of mass and age between main-sequence planet and non-planet hosts may be present.

**Conclusions.** Our results are well explained by radial mixing in the Galaxy. The sample of giant contains stars more massive and younger than their main-sequence counterparts. This leads to a sample of stars possibly less contaminated by stars not born in the solar neighbourhood, leading to no chemical differences between planet and non planet hosts. The sample of main-sequence stars may contain more stars from the outer disc (specially the non-planet host sample) which might led to the differences observed in the chemical trends.

**Key words.** techniques: spectroscopic - stars: abundances -stars: late-type -stars: planetary systems

## 1. Introduction

Detailed chemical analysis of large samples of stars hosting planets have revealed as a powerful technique to help in our understanding of how planetary systems do form and evolve. However, besides the increasing number of recent studies (e.g. Biazzo et al. 2015; da Silva et al. 2015; Maldonado et al. 2015; Nissen 2015; Ramírez et al. 2015; Thiabaud et al. 2015), the only well established correlation found so far is the one that relates the stellar metallicity with the probability of hosting

a gas giant planet (e.g. Gonzalez 1997; Santos et al. 2004; Fischer & Valenti 2005). Any other claim of a chemical trend in planet-hosting stars has so far been disputed.

Meléndez et al. (2009) reports a deficit of refractory elements in the Sun with respect to other solar twins concluding that it is related to the formation of terrestrial planets. Similar chemical patterns are found by Ramírez et al. (2009, 2010) and Gonzalez (2011) in other solar twins and analogs. This interpretation has however been challenged by other works that point towards galactic chemical evolution effects (González Hernández et al. 2010, 2013) or towards an age/inner galactic origin of the planet hosts stars as the cause of the detected small chemical depletions (Adibekyan et al. 2014). In a recent work, Maldonado et al. (2015, hereafter MA15) reports chemical different slopes in the abundance versus elemental condensation temperature diagram between stars with cool gas-giant planets and non-planet hosts, noting as well moderate correlations between the abundance-condensation temperature trend and stellar properties such as age or metallicity.

While most of the detailed chemical studies done so far are around main-sequence (MS) stars, little is known about possi-

Send offprint requests to: J. Maldonado

e-mail: jmaldonado@astropa.inaf.it

\* Based on observations made with the Mercator Telescope; on observations made with the Nordic Optical Telescope; on observations made with the Italian Telescopio Nazionale Galileo; on observations collected at the Centro Astronómico Hispano Alemán (CAHA) at Calar Alto; and on data products from observations made with ESO Telescopes at the La Silla Paranal Observatory under programme ID 072.C-0488(E), 080.D-0347(A), 081.D-0870(A), 087.C-0831(A), and 183.C-0972(A).

\*\* Tables 1, 2, and 3 are only available in the electronic version of the paper or at the CDS via anonymous ftp to cdsarc.u-strasbg.fr (130.79.128.5) or via <http://cdsweb.u-strasbg.fr/cgi-bin/qcat?J/A+A/>

ble chemical trends in evolved stars with planets. For instance, it is still unclear whether giant stars with planets follow the gas-giant planet stellar metallicity correlation (Sadakane et al. 2005; Schuler et al. 2005; Hekker & Meléndez 2007; Pasquini et al. 2007; Takeda et al. 2008; Ghezzi et al. 2010a). With the wealth of new planetary discoveries in the last years we re-visit this issue by performing homogeneous observations and analysis of a large sample of 142 evolved stars. In Maldonado et al. (2013, hereafter MA13), we find that whilst the metallicity distribution of planet-hosting giant stars with stellar masses  $M_{\star} > 1.5 M_{\odot}$  follow the general trend established for the main sequence stars hosting planets, giant planet hosts in the mass domain  $M_{\star} \leq 1.5 M_{\odot}$  do not show metal enrichment. Similar results are found by Mortier et al. (2013). However, Jofré et al. (2015) does not find any clear metallicity difference between giant stars as planet hosts and non hosts for  $M_{\star} > 1.5 M_{\odot}$ . Reffert et al. (2015) explore the planet occurrence rate with stellar metallicity and stellar mass (exploring the mass range 1.0–3.8  $M_{\odot}$ ) in the UCO/Lick survey. The authors perform a distinction between “secure” (15 stars) planet hosts and planet “candidates” (20 stars) based on their available data and found a strong planet-metallicity correlation among the secure planet hosts, and attribute the lack of correlation found on the sample of planet candidates to the fact that the candidate planets are found preferentially among stars with rather small metallicity and mass. The fact that the bulk of their candidate planets is found among their less massive and low-metallicity stars is intriguing at least.

Further, the detection of planetary companions is hampered by the large levels of stellar jitter in evolved stars introduced by stellar p-mode oscillations, which may reach  $\sim 100 \text{ m s}^{-1}$  (Kjeldsen & Bedding 1995). Niedzielski et al. (2016) show that the minimum detectable planetary mass is an increasing function of the orbital separation and the stellar luminosity, being the detection of close-in, small planets ( $M_p \sin i < 2 M_J$  within 1 au) a difficult task when dealing with evolved stars.

In this paper a detailed analysis of the chemical abundances of a large sample of evolved (subgiants and red giants) stars with and without planets is presented. We aim to test whether these stars show any chemical peculiarity, and to unravel their origin. This work follows the analysis presented in MA13, but now we extend it to studying possible trends between the abundances and the elemental condensation temperature. This paper is organised as follows. Sect. 2 describes the stellar samples analysed in this work, the spectroscopic data in which the work is based and the analysis. The distribution of abundances are presented in Sect. 3. The results are discussed in Sect. 4. Our conclusions follow in Sect. 5.

## 2. Data and spectroscopic analysis

### 2.1. Stellar sample

Figure 1 shows the Hertzsprung-Russell (HR) diagram of the observed stars. The total number of stars amounts up to 341. They are classified as red giants (blue triangles), subgiants (red squares), and main-sequence stars (green circles). The samples of giant and subgiant stars were built using as reference the stars listed in MA13, with additional data for twelve new subgiants. The list of MS stars comes from MA13 and M15 works and have been analysed homogeneously. According to their luminosity class and taking into account the presence (or absence) of planetary companions<sup>1</sup>, our sample is divided

<sup>1</sup> According to the available data at the Extrasolar Planets Encyclopaedia, <http://exoplanet.eu/>

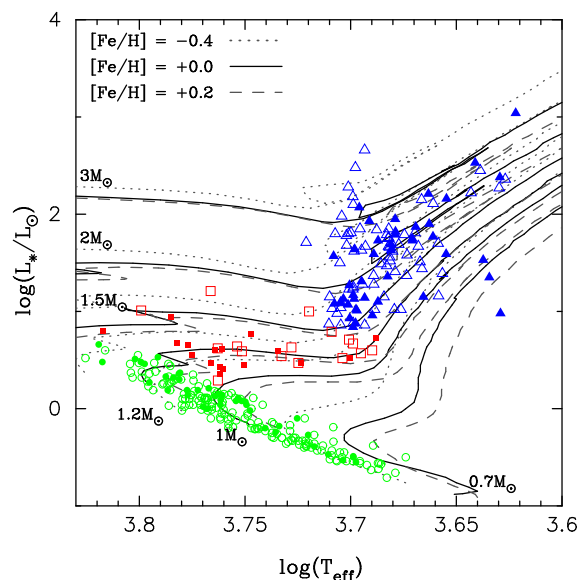


**Fig. 1.** Luminosity versus  $T_{\text{eff}}$  diagram for the observed stars. Giants are plotted with blue triangles, subgiants with red squares, and MS stars with green circles. Filled symbols indicate planet hosts. Some evolutionary tracks ranging from 0.7 to 3.0 solar masses from Girardi et al. (2000) are overplotted. For each mass, three tracks are plotted, corresponding to  $Z=0.008$  ( $[\text{Fe}/\text{H}]=-0.4$  dex, dotted lines),  $Z=0.019$  ( $[\text{Fe}/\text{H}]=+0.0$  dex, solid lines), and  $Z=0.030$  ( $[\text{Fe}/\text{H}]=+0.20$  dex, dashed lines).

into 43 giant stars with known planets (hereafter GWPs), 67 giant stars without planets (GWOPs), 16 subgiants hosting planets (SGWPs), 17 subgiants without planets (SGWOPs), 41 MS stars harbouring planets (MSWPs), and 157 MS stars without known planets (MSWOPs). We note that the total number of giant stars known to host planets is 68 so our GWP sample is statistically representative although it does not include the stellar hosts non-observable from the northern hemisphere.

Before continuing with the analysis we have first checked for the presence of biases in our sample that might influence the results. Recently, Reffert et al. (2015) suggested that previous samples of GWPs may be contaminated by “unsecure” planet detections, mainly around low-metallicity and low-mass stars since this seems to be the case in the sample they analysed. In order to test whether this could be our case, we have checked whether our original sample of stars with planets overlap with the list of planets included in the web-page maintained by these authors<sup>2</sup>. Note that those are radial velocity planets published in the literature and therefore each data set is subject to different selection criteria than that applied to differentiate among secure/candidate planet candidates in the sample of Reffert et al. (2015). Obviously, the criteria used by those authors to include (or not) a planet detection in their web-page may be discussed, but this is out of the scope of this work. Here, we just assumed their criteria is valid and check for biases in our sample. From our original list of 43 GWPs, 27 overlap with the aforementioned list, while 16 are not included in this list. The analysis of the metallicity distribution of secure/unsecure planets hosts, Figure 2 (left), reveals that stars with “unsecure” planets do not show lower metallicities, but rather higher metallicities than the stars with secure planets. While the median metallicity of the secure planets hosts is  $-0.11$  dex, “unsecure” planets hosts show a median value of  $+0.02$  dex. Further, a two-sided Kolmogorov-Smirnov (KS) test

<sup>2</sup> <http://www.lsw.uni-heidelberg.de/users/sreffert/giantplanets.html>

returns a probability of  $\sim 0.1$  of both distributions being drawn from the same parent population. Therefore, we conclude that the metallicity distribution of the 16 planets not included in the Reffert’s list do not seem to contaminate our sample towards low-metallicity stars.

Our GWOP sample was selected based on available giant stars from the Massarotti et al. (2008) list of HIPPARCOS giants within 100 pc from the Sun. So, in principle we cannot rule out the possibility that some of these stars host an undetected gas-giant planet. Reffert et al. (2015) claim planet detection of 4-5% in their sample. A slightly higher detection rate of 10-15% is provided by the Thüringer Landessternwarte survey (Döllinger et al. 2009). Johnson et al. (2011) analyse 246 subgiants from the California Planet Search, providing a detection rate of 15%. These numbers are consistent with the models by Kennedy & Kenyon (2008) which predict a frequency of gas-giant planets of 10% around  $1.5 M_{\odot}$  stars. To test whether our GWOP sample may be contaminated, we divided it into two subsamples: one including those stars which have been monitored in the UCO/Lick survey as listed in Reffert et al. (2015) and have not been reported to have a detected planet (10 stars); and another subsample with our GWOP stars not included in this survey (57 stars). Figure 2 (right), shows the metallicity distribution of both subsamples. From the plot is clear that they are almost identical. A KS test provides a probability of 94% of both subsamples having similar metallicity distributions. Thus, we conclude that it is very unlikely that the properties of our GWOP (such as metallicity or elemental abundances) are affected in a significant way by the presence of undetected gas-giant planets. This result seems in line with the contamination expected in the GWOP sample (as seen, at most at the 10% level), too small to significantly affect the results /shift the metallicity distributions.

Considering less massive planets ( $M_p \sin i < 30 M_{\oplus}$ ), there is increasing evidence that they might be common around MS solar-type stars (e.g. Mayor et al. 2011; Cassan et al. 2012; Howard et al. 2013), which may certainly contaminate the MSWOP sample. We note that stars hosting low-mass planets do not seem to be preferentially metal rich (Ghezzi et al. 2010b; Mayor et al. 2011; Sousa et al. 2011; Buchhave et al. 2012; Buchhave & Latham 2015, although see Wang & Fischer (2015), for an opposing view). Furthermore, MA15 find that stars with low-mass planets show similar chemical trends that stars without known planetary companions. Therefore we discarded from our MSWP sample those stars harbouring low-mass planets.

Regarding giant stars, the detection of low mass planets is hindered around this kind of stars (see e.g. Niedzielski et al. 2016). Therefore any hint of giant stars hosting more massive planets than MS stars (e.g. MA13) needs to be interpreted with caution as the larger levels of stellar oscillation in evolved stars certainly introduce an observational bias against the detection of low-mass planets via the radial velocity method. In addition, it is relevant to note that low-mass planets have more chances of surviving the processes that take place when a MS star evolves off the MS as there is a strong dependence of the tidal forces on the mass ratio of the planet-star system (e.g. Villaver & Livio 2009; Mustill & Villaver 2012; Villaver et al. 2014).

We finally note that the mass distribution of our giant stars is similar to those of more general exoplanet search projects focused on evolved stars (see next subsection for details on this calculation). Our evolved stars sample covers a mass range between  $1.0$  and  $3.6 M_{\odot}$  having a peak at  $\sim 1.5 M_{\odot}$  and then decreases steadily, as does the mass distribution of the giant stars of the

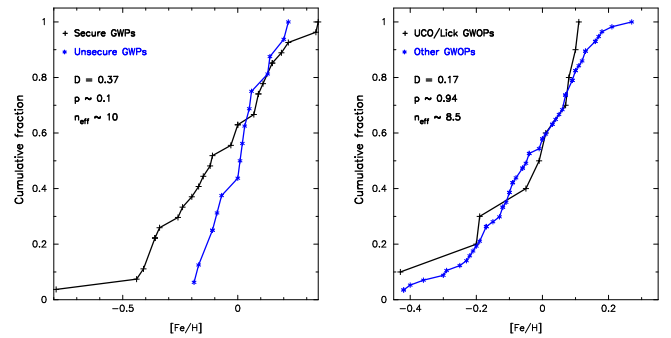


**Fig. 2.** Cumulative [Fe/H] distribution for giant stars. Left: GWOPs, divided into “secure” (27 stars) and “unsecure” (16 stars) planet hosts. Right: GWOPs, divided into stars included in the UCO/Lick survey (10 stars) and GWOPs non-included in this survey (57 stars). See text for details.

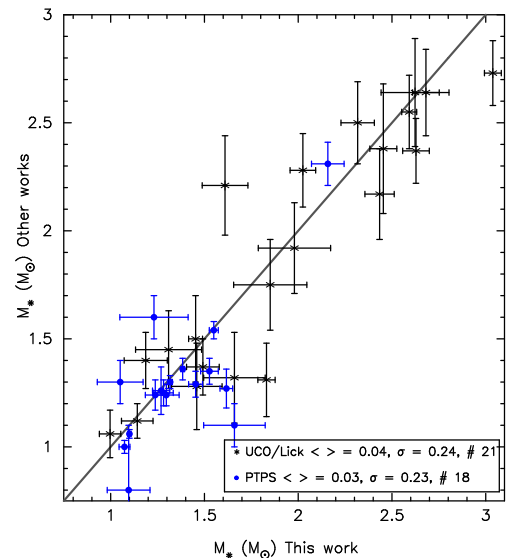


**Fig. 3.** Stellar mass values from the literature estimates versus the values obtained in this work. The symbol  $\langle \rangle$  in the legend represents the median difference. The Gran continuous line represents the 1:1 relation.

PTPS survey or the Retired A Stars project (see Niedzielski et al. 2016, Figure 13c).

Recent works have put into question the reliability of the masses of evolved stars hosting planetary systems (Lloyd 2011, 2013; Schlaufman & Winn 2013). Therefore, a comparison between our derived masses and those given in the PTPS (Zieliński et al. 2012; Niedzielski et al. 2016) and in the UCO/Lick (Reffert et al. 2015) surveys were performed. The masses provided in other surveys might be overestimated (see Niedzielski et al. 2016) and thus we do not use them for comparison with our sample. The Retired A stars and their Companions survey (Ghezzi & Johnson 2015) also provides masses consistent with the PTPS and Lick surveys, however, we do not have enough stars in common to include them in the analysis. The comparison is shown in Figure 3. It reveals an overall good agreement between our mass estimates and those by PTPS and Lick surveys. Note that the median difference is only 0.03, 0.04 solar masses with a rms standard deviation of 0.23, and 0.24  $M_{\odot}$  for the PTPS and Lick surveys respectively.



## 2.2. Spectroscopic analysis

The spectroscopic data used in this work is basically the same used in MA13 and MA15 to which we refer to for further details. In brief, high-resolution spectra of the stars were obtained: i) at La Palma observatory (Canary Islands, Spain) with the HERMES spectrograph (Raskin et al. 2011) at the MERCATOR telescope; ii) at the Nordic Optical Telescope with the FIES (Frandsen & Lindberg 1999) instrument; iii) at the 2.2-metre telescope of the Calar Alto observatory (CAHA, Almería, Spain) using the the FOCES (Pfeiffer et al. 1998) spectrograph; iv) at the Telescopio Nazionale Galileo (TNG, 3.58 m) using the SARG (Gratton et al. 2001) spectrograph. Additional spectra from the public library “S<sup>4</sup>N” (Allende Prieto et al. 2004) as well as HARPS and FEROS spectra from the ESO Archive Facility<sup>3</sup> were also used.

We are aware that ideally, all our targets should have been observed with the same spectrograph and configuration. However, all the spectra used in this work have high resolution (from  $\sim 42000$  of FEROS spectra to  $\sim 115000$  for HARPS), have a high signal-to-noise ratio (median value 107 at 6050 Å) and cover a wide spectral range (from 3780-6910 Å for HARPS to 3400-10900 Å for McDonald) with enough lines for a high-quality abundance determination.

Basic stellar parameters  $T_{\text{eff}}$ ,  $\log g$ , microturbulent velocity  $\xi_t$ , and [Fe/H] are determined using the code TGVIT<sup>4</sup> (Takeda et al. 2005), which implements the iron ionisation and excitation equilibrium conditions, a methodology widely applied to solar-like stars. The line list as well as the adopted parameters (excitation potential,  $\log(gf)$  values) can be found on Y. Takeda’s web page. This code makes use of ATLAS9, plane-parallel, LTE atmosphere models (Kurucz 1993).

Chemical abundance of individual elements C, O, Na, Mg, Al, Si, S, Ca, Sc, Ti, V, Cr, Mn, Co, Ni, and Zn were obtained using the 2014 version of the code MOOG<sup>5</sup> (Snedden 1973) together with ATLAS9 atmosphere models (Kurucz 1993). The measured equivalent widths (EWs) of a list of narrow, non-blended lines for each of the aforementioned species are used as inputs. The selected lines are taken from the list provided by MA15. Hyperfine structure (HFS) was taken into account for V I, and Co I abundances. HFS corrections for Mn I were not taken into account as in MA15 we found slightly different abundances when considering different lines. Although HFS effects may be present for other elements (e.g. Mg I, Sc I), we do not expect these effects to bias the results of the comparisons performed in this work between samples of stars with and without planets, given that they have otherwise similar properties.

The oxygen abundance was derived from the forbidden [O I] line at 6300 Å. This line is well known to be blended with a closer Ni I line (e.g. Allende Prieto et al. 2001). We made use of the MOOG driver *ewfind* to determine the EW of the Ni line using the previously derived Ni abundance. This EW was subtracted from the measured EW of the of the Ni I plus [O I] feature. Then, the oxygen abundance was determined from the remaining EW (e.g. Delgado Mena et al. 2010; González Hernández et al. 2013). Since oxygen abundances in MA15 stars were derived from the O I triplet lines at 777 nm, we have recomputed them using the [O I] 630 nm line. For the carbon abundance the lines at 505.2 and 538.0 nm were used instead of those reported in MA15, since we found the latest

**Table 4.** Results of the  $\langle[X/Fe]\rangle$ - $T_C$  linear fits. For each fit its probability of slope “being by chance” ( $p$ ) is also given.

Sample	All elements		Only refractory	
	slope ( $\times 10^{-5}$ dex/K)	$p$	slope ( $\times 10^{-5}$ dex/K)	$p$
GWPs	$-5.31 \pm 1.20$	0.06	$-6.19 \pm 1.84$	0.07
GWOPs	$-4.14 \pm 0.81$	0.07	$-13.14 \pm 1.45$	0.05
SGWPs	$2.24 \pm 1.17$	0.12	$-3.06 \pm 2.32$	0.17
SGWOPs	$0.36 \pm 1.29$	0.17	$5.66 \pm 3.35$	0.17
MSWPs	$-2.27 \pm 1.11$	0.11	$-5.14 \pm 1.53$	0.13
MSWOPs	$-1.03 \pm 0.79$	0.08	$2.31 \pm 1.32$	0.19

to give abnormally high abundances for the giant stars. Some problems when using the 505.2 nm line have been reported by da Silva et al. (2011). However, we do not find significant differences between the abundances derived from the 505.2 nm line and the ones derived from the 538.0 nm line, being the mean and median differences around  $\sim 0.02$ .

Evolutionary parameters namely, stellar mass, radius, and age were computed using the code PARAM<sup>6</sup> (da Silva et al. 2006) with the new PARSEC isochrones from Bressan et al. (2012).

Our derived stellar parameters are given in Table 1, whilst the abundances are provided in Table 2. The recomputed abundances of carbon and oxygen for those stars taken from MA15 are given in Table 3. These tables are available at the CDS.

## 3. Analysis

### 3.1. $[X/Fe]$ - $T_C$ trends

Chemical differences were searched for by studying possible trends between the abundances,  $[X/Fe]$ , and the elemental condensation temperature,  $T_C$ . Mean abundances for each of the samples were computed, and the  $T_C$ -slope was derived by performing a linear fit, weighting each element by its corresponding star-to-star scatter. Values of  $T_C$  correspond to a 50% equilibrium condensation temperature for a solar system composition gas (Lodders 2003).

As in MA15 we compute the slope of the  $[X/Fe]$  vs.  $T_C$  fit considering firstly all refractory and volatile elements ( $T_C^{\text{all}}$ -slope), and then considering only refractories ( $T_C^{\text{refrac}}$ -slope). In this way we take into account the fact that the abundances of volatiles are in general more difficult to obtain accurately<sup>7</sup>. To give a significance for the derived slopes a Monte Carlo simulation was carried out. We created  $10^4$  series of simulated random abundances and errors, keeping the media and the standard deviation of the original data. For each series of simulated data the corresponding  $T_C$ -slope was derived. Assuming that the distribution of the simulated slopes follows a Gaussian function we then compute the probability that the simulated slope takes the value found when fitting the original data (hereafter  $p$ -value). The corresponding plots are shown in Figure 4, and a summary of the fits is presented in Table 4.

Left panel in Figure 4 shows that when all elements are considered there seems to be no difference in the chemical behaviour of the planet host samples with respect to their respective comparison samples. This result holds independently of the evolutionary state of the stars (giant, subgiant or main-sequence), showing stars with and without planets very similar slopes. We note however that the slopes of MS and subgiant stars tend, within the errors, to be consistent with zero, with moderate  $p$ -

<sup>3</sup> [http://archive.eso.org/wdb/wdb/adp/phase3\\_main/form](http://archive.eso.org/wdb/wdb/adp/phase3_main/form)

<sup>4</sup> <http://optik2.mtk.nao.ac.jp/~takeda/tgv/>

<sup>5</sup> <http://www.as.utexas.edu/~chris/moog.html>

<sup>6</sup> <http://stev.oapd.inaf.it/cgi-bin/param>

<sup>7</sup> We consider as volatile those elements with  $T_C$  lower than 900 K, namely C, O, S, and Zn.

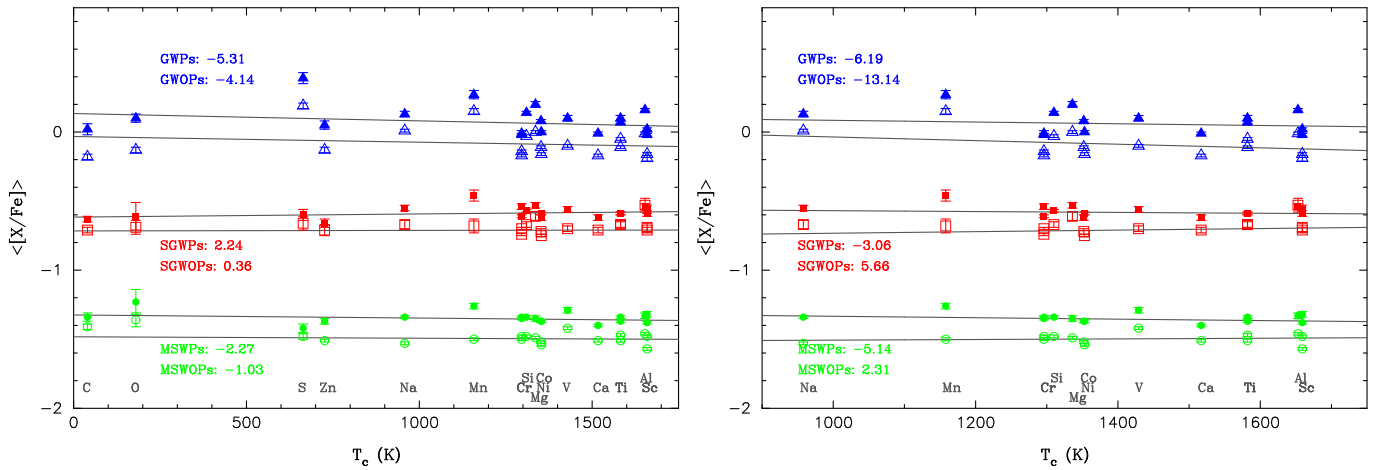


**Fig. 4.**  $\langle [X/Fe] \rangle$ - $T_c$  trends of all the stars analysed. Giants are plotted with blue triangles, subgiants with red squares, and MS stars with green circles. Filled symbols indicate planet hosts. Each planet host subsample is shown against its corresponding comparison subsample (e.g. GWPs vs. GWOPs) with an offset of -0.15 for the sake of clarity. The offset between giants, subgiants, and MS samples is -0.75. For guidance, the derived slopes are shown in the plots (units of  $10^{-5}$  dex/K). The left panel shows the  $\langle [X/Fe] \rangle$ - $T_c$  trends when all elements (volatiles and refractories) are taken into account whilst the right one shows the  $\langle [X/Fe] \rangle$ - $T_c$  trends when only refractories are considered.

values. Giants, on the other hand, show clearly negative slopes and statistically significant low  $p$ -values.

The  $[X/Fe]$  vs.  $T_c$  trends when only refractory elements are considered are shown in the right panel of Figure 4. We note a slight change in behaviour between MSWPs (negative slope) with respect to MSWOPs (positive slope). This tendency is also seen in the samples of subgiant stars (i.e., negative slopes in planet hosts, positive slopes in non-planet hosts). The statistical significance of these trends is however low, with moderate  $p$ -values. When considering giant stars both GWP and GWOP samples show negative  $[X/Fe]$  vs.  $T_c$  trends, being the slope of the GWOP sample slightly more negative. Note that the slopes obtained for the giant samples are statistical significant but that is not the case for the MS and subgiant samples.

We also note that at this point we are considering the sample of giants as a whole, i.e., without any mass differentiation, despite the reported difference in the metallicity behaviour between stars with masses lower and larger than  $1.5 M_{\odot}$ . We will analyse the mass segregation in detail in Section 3.3. We caution that other effects (e.g. uncertainties in the stellar mass determination, or the criteria used to discern subgiants from giants) may also be present.

### 3.2. Trends with evolutionary properties

In the previous subsection we have found that a different chemical trend may exist between planets and non-planets hosts when only refractory elements are considered, but that this difference seem to be only present in MS and subgiant stars, and not in giants. This behaviour resembles the gas-giant planet-metallicity correlation known to hold for MS and subgiant stars but controversial when considered giants (e.g. MA13). It is, therefore, natural to ask whether the obtained abundance trends correlate with other evolutionary parameter.

We have thus performed a search for correlations between the derived  $T_c$ -slopes for each individual star and the evolutionary parameters namely- surface gravity, stellar mass, age, and radius. Stellar metallicity and the stellar mean galactocentric distance ( $d_{\text{galact}}$ ) have been as well considered with values taken from our own previous work and from Casagrande et al. (2011) respectively. Two kinds of analysis have been performed. The

first one consists on the classical Spearman's correlation test. Further analysis includes the evaluation of the significance of the correlations by a bootstrap Monte Carlo (MC) test plus a Gaussian random shift of each data-point within its error bars. The tests were done using the code MCSPEARMAN<sup>8</sup> by Curran (2014) and the results are shown in Table 5. It is clear from this table that the classical analysis suggests moderate but highly significant correlations between the  $T_c$ -slopes and the evolutionary parameters. The MC simulations do not exclude such dependencies, however suggest that the correlations are weak, being the z-score values in all cases lower than  $3\sigma$ .

Our analysis show that the derived  $T_c$ -slope correlates with the stellar metallicity. Such a correlation suggests that Galactic Chemical Evolution (GCE) effects may be impacting our derived abundance patterns. While some authors (González Hernández et al. 2013; Adibekyan et al. 2014) have tried to account for these effects by fitting straight lines to the  $[X/Fe]$  vs.  $[Fe/H]$  plots, others (e.g. Ramírez et al. 2014) argue that correcting from GCE effects in this manner may prevent us from finding elemental depletions due to planet formation.

Table 5 also shows a clear correlation between the  $T_c$ -slope and the stellar mass, or the stellar age (see the corresponding  $p$ -values). We note that the correlations were performed using all stars (planet and non planet hosts) together. Less massive and older stars show more positive  $T_c^{\text{ref}}$ -slopes, and more negative  $T_c^{\text{all}}$ -slopes. This result agree with recent studies of solar twins in which the existence of a correlation between  $[X/Fe]$  and the stellar age have been revealed (Nissen 2015; Spina et al. 2016). Following this line of reasoning, a comparison of the stellar masses and ages between planet hosts and non planet hosts were performed. Figure 5 and 6 show the corresponding cumulative distribution functions, while some statistical diagnostics are presented in Table 6. These figures show that there seems to be a hint of MS and subgiant non-planet hosts to have slightly smaller masses and older ages than planet hosts. This could be a selection effect as radial velocity surveys tend to target stars with low levels of activity. We note that for the case of giants the behaviour seems to be the opposite, being GWOPs slightly younger and massive than GWPs.

<sup>8</sup> <https://github.com/PACurran/MCSpearman/>

**Table 5.** Results from the Spearman’s correlation test between the  $T_C$  slopes and different stellar properties. MC stands for Monte Carlo simulation, CA for “classical” analysis, SR for Spearman’s correlation rank coefficient, ZS means z-score, and  $p$  denotes the significance of the SR coefficient.

Parameter	Sample	All elements				Only refractory			
		MC		CA		MC		CA	
		SR	ZS	SR	$p$	SR	ZS	SR	$p$
[Fe/H]	All	$0.29 \pm 0.05$	$2.29 \pm 0.45$	0.31	$\sim 10^{-8}$	$-0.32 \pm 0.05$	$-2.57 \pm 0.45$	-0.37	$\sim 10^{-12}$
	Giants	$0.44 \pm 0.09$	$2.10 \pm 0.47$	0.48	$\sim 10^{-7}$	$-0.42 \pm 0.09$	$-1.96 \pm 0.45$	-0.51	$\sim 10^{-8}$
	Subgiants	$0.49 \pm 0.15$	$1.30 \pm 0.49$	0.52	$\sim 10^{-3}$	$-0.55 \pm 0.15$	$-1.48 \pm 0.52$	-0.60	$\sim 10^{-4}$
	MS	$0.15 \pm 0.07$	$0.92 \pm 0.43$	0.16	0.02	$-0.28 \pm 0.07$	$-1.69 \pm 0.45$	-0.32	$\sim 10^{-6}$
logg	All	$-0.16 \pm 0.05$	$-1.27 \pm 0.44$	-0.18	$\sim 10^{-3}$	$0.22 \pm 0.05$	$1.75 \pm 0.44$	0.28	$\sim 10^{-7}$
	Giants	$0.26 \pm 0.10$	$1.17 \pm 0.45$	0.28	$\sim 10^{-3}$	$0.17 \pm 0.10$	$0.74 \pm 0.43$	0.22	0.02
	Subgiants	$0.30 \pm 0.17$	$0.75 \pm 0.45$	0.33	0.06	$-0.33 \pm 0.17$	$-0.82 \pm 0.45$	-0.36	0.04
	MS	$-0.17 \pm 0.07$	$-1.00 \pm 0.41$	-0.19	$\sim 0.01$	$0.16 \pm 0.07$	$0.98 \pm 0.44$	0.21	$\sim 10^{-3}$
$M_\star$	All	$0.34 \pm 0.05$	$2.70 \pm 0.43$	0.36	$\sim 10^{-11}$	$-0.37 \pm 0.05$	$-2.97 \pm 0.45$	-0.45	$\sim 10^{-17}$
	Giants	$0.43 \pm 0.08$	$2.00 \pm 0.43$	0.50	$\sim 10^{-8}$	$-0.57 \pm 0.07$	$-2.84 \pm 0.48$	-0.70	$\sim 10^{-17}$
	Subgiants	$0.29 \pm 0.17$	$0.71 \pm 0.42$	0.32	0.08	$-0.23 \pm 0.19$	$-0.55 \pm 0.47$	-0.25	0.17
	MS	$0.31 \pm 0.07$	$1.87 \pm 0.45$	0.33	$\sim 10^{-6}$	$-0.32 \pm 0.07$	$-1.96 \pm 0.46$	-0.39	$\sim 10^{-8}$
Age	All	$-0.11 \pm 0.06$	$-0.82 \pm 0.43$	-0.14	$\sim 0.01$	$0.25 \pm 0.05$	$1.94 \pm 0.44$	0.31	$\sim 10^{-8}$
	Giants	$-0.35 \pm 0.09$	$-1.62 \pm 0.43$	-0.47	$\sim 10^{-7}$	$0.52 \pm 0.08$	$2.52 \pm 0.49$	0.65	$\sim 10^{-14}$
	Subgiants	$-0.31 \pm 0.16$	$-0.76 \pm 0.42$	-0.35	0.05	$0.10 \pm 0.20$	$0.23 \pm 0.49$	0.11	0.54
	MS	$-0.02 \pm 0.07$	$-0.10 \pm 0.42$	-0.03	0.72	$0.15 \pm 0.07$	$0.86 \pm 0.42$	0.17	0.02
$R_\star$	All	$0.23 \pm 0.05$	$1.79 \pm 0.44$	0.25	$\sim 10^{-6}$	$-0.27 \pm 0.05$	$-2.09 \pm 0.45$	-0.33	$\sim 10^{-9}$
	Giants	$-0.11 \pm 0.10$	$-0.48 \pm 0.45$	-0.11	0.27	$-0.31 \pm 0.09$	$-1.41 \pm 0.43$	-0.39	$\sim 10^{-5}$
	Subgiants	$-0.19 \pm 0.19$	$-0.44 \pm 0.46$	-0.22	0.22	$0.13 \pm 0.18$	$0.32 \pm 0.43$	0.14	0.43
	MS	$0.29 \pm 0.07$	$1.74 \pm 0.45$	0.31	$\sim 10^{-5}$	$-0.24 \pm 0.07$	$-1.41 \pm 0.46$	-0.29	$\sim 10^{-5}$
$d_{\text{galact}}$	All	$0.00 \pm 0.08$	$0.03 \pm 0.44$	0.00	0.99	$-0.21 \pm 0.07$	$-1.20 \pm 0.44$	-0.22	$\sim 10^{-3}$

**Table 6.** Stellar mass and stellar age statistics of the stellar samples.

Stellar mass ( $M_\odot$ )					
Sample	Mean	Median	$\sigma$	Min.	Max.
MSWPs	1.06	1.03	0.16	0.79	1.48
MSWOPs	0.95	0.94	0.14	0.68	1.37
SGWPs	1.25	1.30	0.13	1.03	1.49
SGWOPs	1.24	1.19	0.22	0.93	1.62
GWPs	1.60	1.48	0.48	1.01	3.04
GWOPs	1.76	1.60	0.56	1.00	3.62
Stellar age (Gyr)					
Sample	Mean	Median	$\sigma$	Min.	Max.
MSWPs	3.41	3.02	2.41	0.29	9.99
MSWOPs	4.32	3.28	3.62	0.10	11.48
SGWPs	5.00	4.32	1.98	1.01	8.63
SGWOPs	5.62	4.76	2.88	2.01	11.48
GWPs	3.37	2.95	2.15	0.38	10.10
GWOPs	2.82	2.29	2.15	0.24	9.28

In order to test the statistical significance of these trends several KS tests were performed (Table 7). The results from the KS test show that the differences in mass or age between planet and non-planet hosts are in general not significant from an statistical point of view. The mass segregation between planets and non-planet hosts in MS stars appears to be the only trend that might be statistically significant.

In order to check whether GCE effects may affect or not our results, abundances were corrected by fitting straight lines to the [X/Fe] vs. [Fe/H] plots (see Figure A.1). As before,  $T_C$ -slopes were computed for each individual star and a search for correlations was performed. We find that most of the correlations with the evolutionary parameters remain.

**Table 7.** Results of the K-S tests performed in this work. We consider a confidence level of 98% in order to reject the null hypothesis  $H_0$  (both samples coming from the same underlying continuous distribution).

Stellar mass						
Sample	$n_{\text{planets}}$	$n_{\text{comparison}}$	$n_{\text{eff}}$	$D$	$p$	$H_0^\ddagger$
MS	41	151	32	0.36	$\sim 10^{-4}$	1
Subgiants	17	15	7	0.24	0.69	0
Giants	43	67	26	0.22	0.15	0
Stellar age						
Sample	$n_{\text{planets}}$	$n_{\text{comparison}}$	$n_{\text{eff}}$	$D$	$p$	$H_0^\ddagger$
MS	41	151	32	0.18	0.24	0
Subgiants	17	15	7	0.17	0.95	0
Giants	43	67	26	0.22	0.15	0

**Notes.**  $D$  is the maximum deviation between the empirical distribution function of samples 1 and 2.  $p$  corresponds to the estimated likelihood of the null hypothesis, a value that is known to be reasonably accurate for sample sizes for which  $n_{\text{eff}} \geq 4$ .  $^\ddagger$  (0): Accept null hypothesis; (1): Reject null hypothesis.

Finally, we have redone our analysis but considering only those stars similar to our Sun (the so-called solar analogs). Results are given in Table 8. We note that the correlations discussed before are not so evident. However, the classical analysis suggests that some correlations may still be present. In particular between  $T_C^{\text{all}}$  and logg, and perhaps the stellar age, and between  $T_C^{\text{ref}}$  and [Fe/H]. A more detailed strictly differential analysis of these stars should be done to clarify this point and to properly compare with previous results (e.g. Adibekyan et al. 2014; da Silva et al. 2015).

### 3.3. Mass segregation in giants and abundance trends

MA13 find that for giant stars as a whole there is no correlation between the presence of giant planets and the metallicity of the

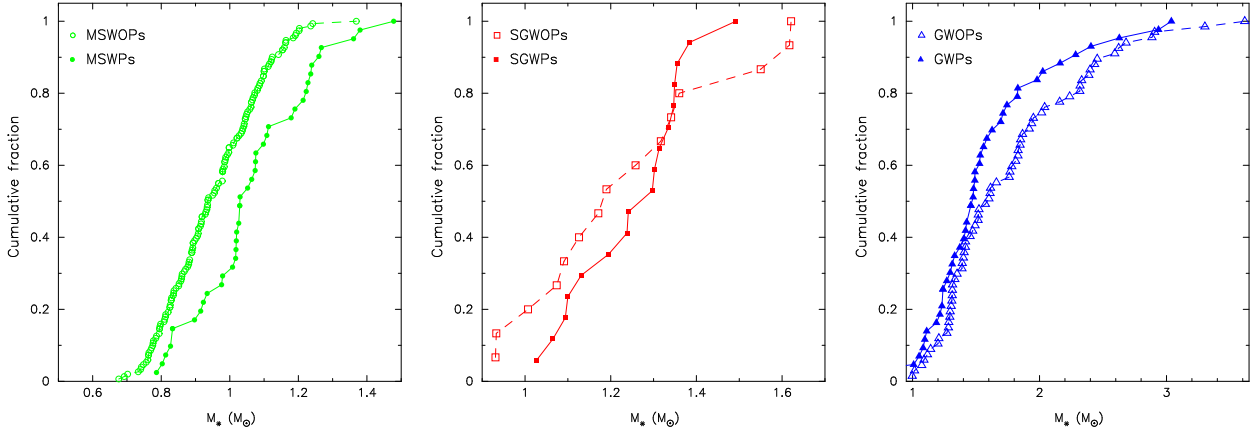


**Fig. 5.** Cumulative distribution function of stellar masses for MS stars (left), subgiants (middle), and giants (right).

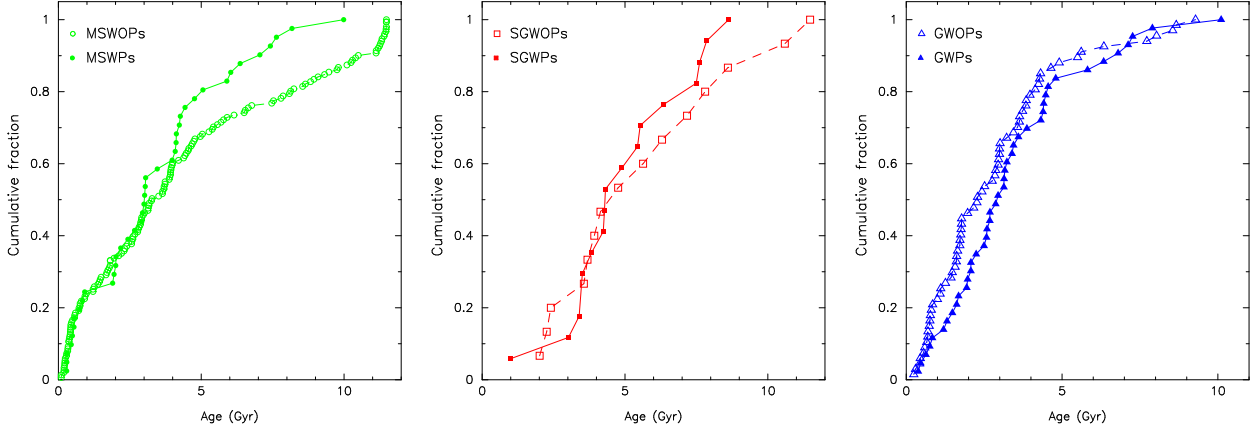


**Fig. 6.** Cumulative distribution function of the stellar age for MS stars (left), subgiants (middle), and giants (right).

**Table 8.** Same as Table 5 but for a sample of 34 solar analogs ( $T_{\text{eff}} = 5777 \pm 200$  K,  $\log g = 4.44 \pm 0.20$  dex,  $[\text{Fe}/\text{H}] = 0.00 \pm 0.20$  dex).

Parameter	All elements					Only refractory				
	<i>MC</i>		<i>CA</i>			<i>MC</i>		<i>CA</i>		
	SR	ZS	SR	<i>p</i>	SR	ZS	SR	<i>p</i>		
[Fe/H]	$0.07 \pm 0.18$	$0.18 \pm 0.44$	$0.06$	$0.72$	$-0.38 \pm 0.15$	$-0.96 \pm 0.43$	$-0.48$	$\sim 10^{-3}$		
logg	$0.32 \pm 0.15$	$0.79 \pm 0.40$	$0.44$	$0.01$	$-0.02 \pm 0.17$	$-0.05 \pm 0.42$	$0.04$	$0.81$		
$M_*$	$0.13 \pm 0.17$	$0.32 \pm 0.42$	$0.13$	$0.47$	$-0.18 \pm 0.18$	$-0.45 \pm 0.44$	$-0.22$	$0.20$		
Age	$-0.22 \pm 0.16$	$-0.53 \pm 0.40$	$-0.29$	$0.10$	$0.08 \pm 0.18$	$0.20 \pm 0.43$	$0.06$	$0.72$		
$R_*$	$-0.16 \pm 0.18$	$-0.38 \pm 0.43$	$-0.20$	$0.26$	$0.11 \pm 0.18$	$0.26 \pm 0.43$	$0.09$	$0.62$		
$d_{\text{galact}}$	$-0.04 \pm 0.18$	$-0.10 \pm 0.43$	$-0.05$	$0.77$	$-0.13 \pm 0.18$	$-0.33 \pm 0.46$	$-0.15$	$0.39$		

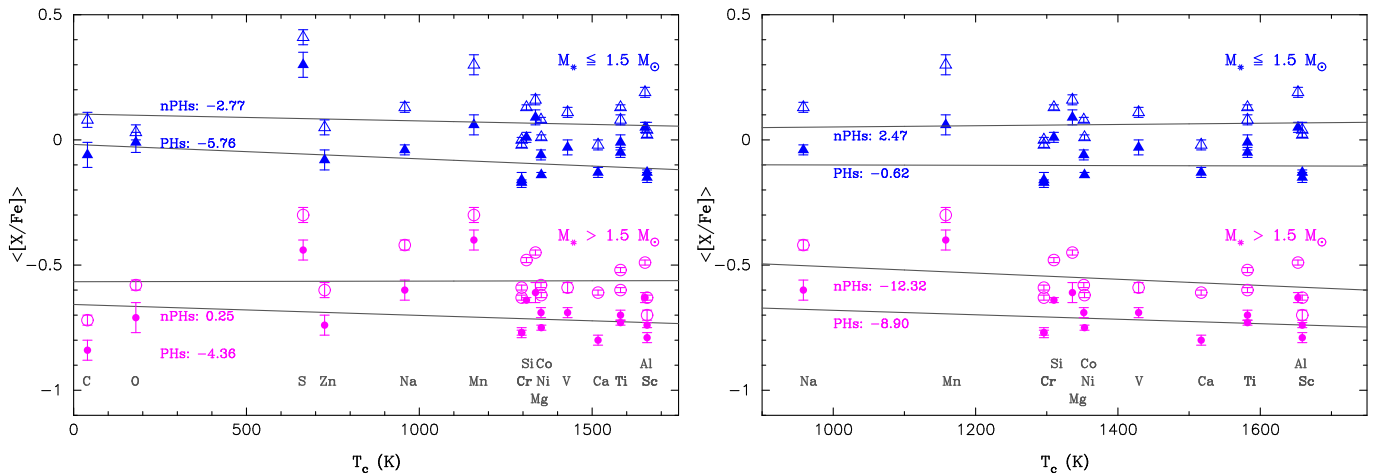
star. However, within the lack of correlation there seems to be hidden a dependency on the stellar mass. While the less massive giant stars with planets ( $M_* \leq 1.5 M_\odot$ ) are not metal rich, the metallicity of the sample of massive ( $M_* > 1.5 M_\odot$ ) giant stars with planets is higher than that of a similar sample of stars without planets. It is therefore natural to ask whether there are no differences in the  $\langle [X/\text{Fe}] \rangle - T_C$  trends between stars more massive than  $1.5 M_\odot$  and less massive giants.

Figure 7 shows the mean  $\langle [X/\text{Fe}] \rangle - T_C$  trend of GWPs and GWOPs for giants with  $M_* \leq 1.5 M_\odot$  and giants in the mass domain  $M_* > 1.5 M_\odot$ . The results of the corresponding linear fits are given in Table 9. We find that when considering all elements, the slopes are always negative with the only exception of the GWOP sample for  $M_* > 1.5 M_\odot$ . However, we note that in this case the slope is consistent with zero. When considering only refractory elements, for the more massive giants, stars with and without planets show similar negative slopes. For giants in

the mass domain  $M_* \leq 1.5 M_\odot$ , GWPs show a slightly negative slope, whilst GWOP a slightly positive one. However, we note that both slopes within their corresponding errors are compatible with zero. We conclude that giant stars do not show differences in the  $\langle [X/\text{Fe}] \rangle - T_C$  trends between planet and not planet hosts. This result holds independently of whether all giants are considered (Section 3.1) or we separate the sample according to the stellar mass.

We note that giants in the mass domain  $M_* \leq 1.5 M_\odot$  show more positive  $\langle [X/\text{Fe}] \rangle - T_C^{\text{ref}}$  slopes than giants with  $M_* > 1.5 M_\odot$ . This fact could in principle be explained by the anticorrelation between the stellar mass and the  $T_C^{\text{ref}}$ -slope seen in the previous subsection. Further, could be hidden within as MA13 pointed out that giants in the mass domain  $M_* \leq 1.5 M_\odot$  show lower metallicities than giants with  $M_* > 1.5 M_\odot$ . Note that the  $T_C^{\text{ref}}$ -slope was shown before to depend on the stellar metallicity.





**Fig. 7.**  $\langle [X/Fe] \rangle$ - $T_C$  trends for the giant stars. GWPs with  $M_\star > 1.5 M_\odot$  are plotted with purple circles, GWPs less massive than  $1.5 M_\odot$  in blue triangles. Filled symbols indicate planet hosts. Each planet host subsample is shown against its corresponding comparison subsample with an offset of -0.15 for the sake of clarity. The offset between the sample of giants with  $M_\star > 1.5 M_\odot$  and less massive giants is -0.75. For guidance, the derived slopes are shown in the plots (units of  $10^{-5}$  dex/K). The left panel shows the  $\langle [X/Fe] \rangle$ - $T_C$  trends when all elements (volatiles and refractories) are taken into account whilst the right one shows the  $\langle [X/Fe] \rangle$ - $T_C$  trends when only refractories are considered.

**Table 9.** Results of the  $\langle [X/Fe] \rangle$ - $T_C$  linear fits for the giant stars according to their masses. For each fit its probability of slope “being by chance” ( $p$ ) is also given.

Sample	All elements		Only refractory	
	slope ( $\times 10^{-5}$ dex/K)	$p$ .	slope ( $\times 10^{-5}$ dex/K)	$p$
$M_\star > 1.5 M_\odot$				
GWPs	$-4.36 \pm 1.58$	0.08	$-8.90 \pm 2.42$	0.06
GWOPs	$0.25 \pm 0.89$	0.05	$-12.32 \pm 1.82$	0.05
$M_\star \leq 1.5 M_\odot$				
GWPs	$-5.76 \pm 1.58$	0.09	$-0.62 \pm 2.35$	0.10
GWOPs	$-2.77 \pm 1.20$	0.08	$2.47 \pm 2.12$	0.07

#### 4. Discussion

In the previous section we have shown that stellar  $T_C$ -slopes correlate with the stellar evolutionary parameters. The data suggest that there might be a different behaviour in the  $\langle [Fe/H] \rangle$ - $T_C$  trends between planets and non planet hosts for MS, and sub-giant stars. However, there seem to be no difference between planet and non planet hosts among the sample of giants.

The finding that the MS non-planet hosts of our sample are less massive and perhaps older than the planet hosts is, if significant, somehow surprising, and might hide some bias in the subsample selection. In fact, spectroscopic targets for planet searches are often deliberately chosen in order to be slow rotators and typically inactive which should sample a population of MS stars older than the average population of the same spectral type. Recently, Bonfanti et al. (2015) have analysed whether exoplanet hosts are peculiar with respect to field stars not hosting planets regarding ages and found that both samples are homogeneous within the solar neighbourhood with a median age distribution of 4.8 Gyr slightly older than the average thin disc population. This seems to be at odds with our results, although it may be an effect of the sample selection. Note that our MS stars are younger on average (See Table 6). Further, the only difference between MSWPs and MSWOPs found to be statistically significant is in the stellar mass.

Haywood (2009) suggested that the observed correlation between the presence of gas-giant planets and enhanced stellar metallicity observed in MS planet hosts might be related to a possible inner-disc origin of these stars. The fact that stars with low-mass planets do not show the metal-rich signature does not

necessary contradict this idea, although further investigations are needed to clarify this point. Radial mixing is a secular process, and its effect is known to increase with time, older stars migrate further and come from a region with significantly different abundances. On the other hand, age and mass are related quantities. MS non-planet host may show a different  $[X/Fe]$ - $T_C$  trends (with respect to planet host) just simply because these stars are slightly older and less massive, and possibly more contaminated by stars from the outer disc. Stars from the outer disc (at larger galactocentric distances) are expected to show lower metallicities (e.g. Lemasle et al. 2008, Figure 5) and therefore larger  $[X/Fe]$  values for most elements (see Figure A.1), which may explain their positive  $T_C^{\text{ref}}$  slopes. In this framework, the lack of a difference between GWPs and GWOPs is explained by the fact that these samples are younger and more massive than their MS counterparts, and therefore significantly less affected by radial mixing.

Along this line, hints of a correlation between the  $T_C$  slopes and the stellar age have already been reported (Adibekyan et al. 2014; Maldonado et al. 2015; Nissen 2015; Spina et al. 2016). Adibekyan et al. (2014) use the stellar mean galactocentric distance as a proxy of the stellar birthplace finding tentative evidence of a correlation with the  $T_C$  slope. Such a correlation seem to be also present in our data (although when considering only refractory elements, see Table 5). Unfortunately, no values of  $d_{\text{galact}}$  are available for most of our giant stars.

An alternative interpretation of the  $\langle [Fe/H] \rangle$ - $T_C$  abundance patterns in planet host was given by Meléndez et al. (2009, hereafter ME09). ME09 report a deficit of refractory elements in the Sun with respect to other solar twins. ME09 conclude that the most likely explanation is related to the formation of planetary systems like our own, in particular to the formation of low-mass rocky planets.

In the analysis performed in Section 3 we have deliberately tried to exclude stars with known low-mass planets from the sample. Nevertheless, a difference between planet hosts and non-planet host is still present in MS stars in the  $T_C^{\text{ref}}$  analysis. This is in line with the results of MA15 where possible differences in abundance trends were found in stars with cool giant-planets, but not in stars with low-mass planets. Since the commonly accepted scenario of gas-giant planets formation requires the previous creation of a rocky core, the hypothesis that the atmospheres of



planet hosts can be contaminated by gas depleted in refractories, may still hold. The contamination of gas depleted in refractories due to the planet formation process needs very accurate timing as the star needs to retain the protoplanetary disc long enough so the planetary signatures are not cleared out by a deep convection zone on the star. Thus as the star evolves off the MS to become a giant this chemical fingerprint should be erased. In principle at the base of the Red Giant Branch phase most of the envelope should be fully convective. In this scenario subgiant stars are expected to show similar chemical fingerprint of planet formation as MS stars but giant stars should have it erased as planet hosts.

However, Figure 4 (right) shows that the sample of stars that show hints of changing its chemical behaviour is the one without planets (from positive slopes for MSWOPs and SGWOPs to negative slopes for GWOPs). Thus, other explanations are required to explain this result. The presence of a galactic radial mixing is in agreement with the fact that we seem to be comparing two different populations of stars, with the stars in the GWOP sample being more massive and younger than stars in the SGWOP and MSWOP samples.

It is important to keep in mind that the stars selected for planet searches around evolved stars are more massive than their MS counterparts (see e.g. Niedzielski et al. 2016) and that it has been shown in MA13 and Reffert et al. (2015) that planet occurrence rate does indeed seem to depend on both, stellar mass and stellar metallicity. The different findings for lower and higher mass stars or MS and evolved systems does not appear to be simply a consequence of a polluted sample of planet hosts with non-planet bearing stars. This explanation put forward by Reffert et al. (2015) is what explains their sample of stars but does not hold in our analysis of a larger sample (3 times larger) even when we account for a possible sample contamination. We find that we are indeed possibly dealing with different populations of stars and we hope that improving sample statistics in the future will allow to better clean the samples to reveal clues on the planet formation process under different conditions.

## 5. Summary

In this work a detailed chemical analysis of a large sample of evolved (subgiants and red giants) with planets has been presented. Their chemical abundances has been compared to those of main-sequence stars.

No clear difference has been found in  $\langle[X/Fe]\rangle$ - $T_C$  trends between planet and non-planet hosts when all elements are considered in the analysis. However, when the analysis is restricted to only refractory elements, planet and non-planet hosts might show different  $T_C$ -slopes. This result holds for subgiant and giant stars, but not for giants.

The data suggest moderate but highly significant correlations between the  $T_C$ -slopes and the stellar evolutionary parameters, namely stellar mass and age. Less massive and older stars show more positive  $T_C^{\text{ref}}$ -slopes and more negative  $T_C^{\text{all}}$ -slopes. In this line, a hint of a difference in terms of mass and age seem to be present among our sample of MS stars although this result should be further investigated, as it seems to be only statistically significant for the stellar mass. We had also found that giants with masses  $M_\star \leq 1.5 M_\odot$  show more positive  $\langle[X/Fe]\rangle$ - $T_C^{\text{ref}}$  slopes than more massive giants, in agreement with their lower masses and metallicities.

Galactic radial mixing offers a suitable scenario for the observed trends. Giant stars are more massive and younger than their MS counterparts and therefore less contaminated by stars

from the outer disc, leading to no chemical differences between planet and non-planet hosts. On the other hand, less massive and older stars in the MSWOP sample may account for different chemical trends between planets and non-planet hosts. Other scenarios invoking the formation of planets do not seem to be supported by our data.

Finally, we note that while general trends between the  $T_C$  slopes and evolutionary parameters may be present, it does not exclude other processes, such as planetary formation, planet engulfment, or dust-gas segregation in protoplanetary disc that may affect the stellar photospheric abundance of refractory elements relative to volatiles (Gaidos 2015; Spina et al. 2016).

*Acknowledgements.* This research was supported by the Italian Ministry of Education, University, and Research through the *PREMALE WOW 2013* research project under grant *Ricerca di pianeti intorno a stelle di piccola massa*. E. V. acknowledges support from the *On the rocks* project funded by the Spanish Ministerio de Economía y Competitividad under grant *AYA2014-55840-P*. Carlos Eiroa is acknowledged for valuable discussions.

## References

- Adibekyan, V. Z., González Hernández, J. I., Delgado Mena, E., et al. 2014, *A&A*, 564, L15
- Allende Prieto, C., Barklem, P. S., Lambert, D. L., & Cunha, K. 2004, *A&A*, 420, 183
- Allende Prieto, C., Lambert, D. L., & Asplund, M. 2001, *ApJ*, 556, L63
- Biazzo, K., Gratton, R., Desidera, S., et al. 2015, *A&A*, 583, A135
- Bonfanti, A., Ortolani, S., Piotto, G., & Nascimbeni, V. 2015, *A&A*, 575, A18
- Bressan, A., Marigo, P., Girardi, L., et al. 2012, *MNRAS*, 427, 127
- Buchhave, L. A. & Latham, D. W. 2015, *ApJ*, 808, 187
- Buchhave, L. A., Latham, D. W., Johansen, A., et al. 2012, *Nature*, 486, 375
- Casagrande, L., Schönrich, R., Asplund, M., et al. 2011, *A&A*, 530, A138
- Cassan, A., Kubas, D., Beaulieu, J.-P., et al. 2012, *Nature*, 481, 167
- Curran, P. A. 2014, ArXiv e-prints [arXiv: 1411.3816]
- da Silva, L., Girardi, L., Pasquini, L., et al. 2006, *A&A*, 458, 609
- da Silva, R., Milone, A. C., & Reddy, B. E. 2011, *A&A*, 526, A71
- da Silva, R., Milone, A. d. C., & Rocha-Pinto, H. J. 2015, *A&A*, 580, A24
- Delgado Mena, E., Israelian, G., González Hernández, J. I., et al. 2010, *ApJ*, 725, 2349
- Döllinger, M. P., Hatzes, A. P., Pasquini, L., Guenther, E. W., & Hartmann, M. 2009, *A&A*, 505, 1311
- Fischer, D. A. & Valenti, J. 2005, *ApJ*, 622, 1102
- Frandsen, S. & Lindberg, B. 1999, in *Astrophysics with the NOT*, ed. H. Karttunen & V. Pirola, 71
- Gaidos, E. 2015, *ApJ*, 804, 40
- Ghezzi, L., Cunha, K., Schuler, S. C., & Smith, V. V. 2010a, *ApJ*, 725, 721
- Ghezzi, L., Cunha, K., Smith, V. V., et al. 2010b, *ApJ*, 720, 1290
- Ghezzi, L. & Johnson, J. A. 2015, *ApJ*, 812, 96
- Girardi, L., Bressan, A., Bertelli, G., & Chiosi, C. 2000, *A&AS*, 141, 371
- Gonzalez, G. 1997, *MNRAS*, 285, 403
- Gonzalez, G. 2011, *MNRAS*, 416, L80
- González Hernández, J. I., Delgado-Mena, E., Sousa, S. G., et al. 2013, *A&A*, 552, A6
- González Hernández, J. I., Israelian, G., Santos, N. C., et al. 2010, *ApJ*, 720, 1592
- Gratton, R. G., Bonanno, G., Bruno, P., et al. 2001, *Experimental Astronomy*, 12, 107
- Haywood, M. 2009, *ApJ*, 698, L1
- Hekker, S. & Meléndez, J. 2007, *A&A*, 475, 1003
- Howard, A. W., Sanchis-Ojeda, R., Marcy, G. W., et al. 2013, *Nature*, 503, 381
- Jofré, E., Petrucci, R., Saffe, C., et al. 2015, *A&A*, 574, A50
- Johnson, J. A., Clanton, C., Howard, A. W., et al. 2011, *ApJS*, 197, 26
- Kennedy, G. M. & Kenyon, S. J. 2008, *ApJ*, 673, 502
- Kjeldsen, H. & Bedding, T. R. 1995, *A&A*, 293 [astro-ph/9403015]
- Kurucz, R. 1993, *ATLAS9 Stellar Atmosphere Programs and 2 km/s grid*. Kurucz CD-ROM No. 13. Cambridge, Mass.: Smithsonian Astrophysical Observatory, 1993., 13
- Lemasle, B., François, P., Piersimoni, A., et al. 2008, *A&A*, 490, 613
- Lloyd, J. P. 2011, *ApJ*, 739, L49
- Lloyd, J. P. 2013, *ApJ*, 774, L2
- Lodders, K. 2003, *ApJ*, 591, 1220
- Maldonado, J., Eiroa, C., Villaver, E., Montesinos, B., & Mora, A. 2015, *A&A*, 579, A20
- Maldonado, J., Villaver, E., & Eiroa, C. 2013, *A&A*, 554, A84

- Massarotti, A., Latham, D. W., Stefanik, R. P., & Fogel, J. 2008, *AJ*, 135, 209
- Mayor, M., Marmier, M., Lovis, C., et al. 2011, *ArXiv e-prints* [arXiv:1109.2497]
- Meléndez, J., Asplund, M., Gustafsson, B., & Yong, D. 2009, *ApJ*, 704, L66
- Mortier, A., Santos, N. C., Sousa, S. G., et al. 2013, *A&A*, 557, A70
- Mustill, A. J. & Villaver, E. 2012, *ApJ*, 761, 121
- Niedzielski, A., Deka-Szymankiewicz, B., Adamczyk, M., et al. 2016, *A&A*, 585, A73
- Nissen, P. E. 2015, *A&A*, 579, A52
- Pasquini, L., Döllinger, M. P., Weiss, A., et al. 2007, *A&A*, 473, 979
- Pfeiffer, M. J., Frank, C., Baumüller, D., Fuhrmann, K., & Gehren, T. 1998, *A&AS*, 130, 381
- Ramírez, I., Asplund, M., Baumann, P., Meléndez, J., & Bensby, T. 2010, *A&A*, 521, A33
- Ramírez, I., Khanal, S., Aleo, P., et al. 2015, *ApJ*, 808, 13
- Ramírez, I., Meléndez, J., & Asplund, M. 2009, *A&A*, 508, L17
- Ramírez, I., Meléndez, J., & Asplund, M. 2014, *A&A*, 561, A7
- Raskin, G., van Winckel, H., Hensberge, H., et al. 2011, *A&A*, 526, A69
- Reffert, S., Bergmann, C., Quirrenbach, A., Trifonov, T., & Künstler, A. 2015, *A&A*, 574, A116
- Sadakane, K., Ohnishi, T., Ohkubo, M., & Takeda, Y. 2005, *PASJ*, 57, 127
- Santos, N. C., Israelian, G., & Mayor, M. 2004, *A&A*, 415, 1153
- Schlaufman, K. C. & Winn, J. N. 2013, *ApJ*, 772, 143
- Schuler, S. C., Kim, J. H., Tinker, Jr., M. C., et al. 2005, *ApJ*, 632, L131
- Snedden, C. A. 1973, PhD thesis, THE UNIVERSITY OF TEXAS AT AUSTIN.
- Sousa, S. G., Santos, N. C., Israelian, G., Mayor, M., & Udry, S. 2011, *A&A*, 533, A141
- Spina, L., Meléndez, J., & Ramírez, I. 2016, *A&A*, 585, A152
- Takeda, Y., Ohkubo, M., Sato, B., Kambe, E., & Sadakane, K. 2005, *PASJ*, 57, 27
- Takeda, Y., Sato, B., & Murata, D. 2008, *PASJ*, 60, 781
- Thiabaud, A., Marboeuf, U., Alibert, Y., Leya, I., & Mezger, K. 2015, *A&A*, 580, A30
- Villaver, E. & Livio, M. 2009, *ApJ*, 705, L81
- Villaver, E., Livio, M., Mustill, A. J., & Siess, L. 2014, *ApJ*, 794, 3
- Wang, J. & Fischer, D. A. 2015, *AJ*, 149, 14
- Zieliński, P., Niedzielski, A., Wolszczan, A., Adamów, M., & Nowak, G. 2012, *A&A*, 547, A91

## Appendix A: Abundance ratios as a function of stellar metallicity

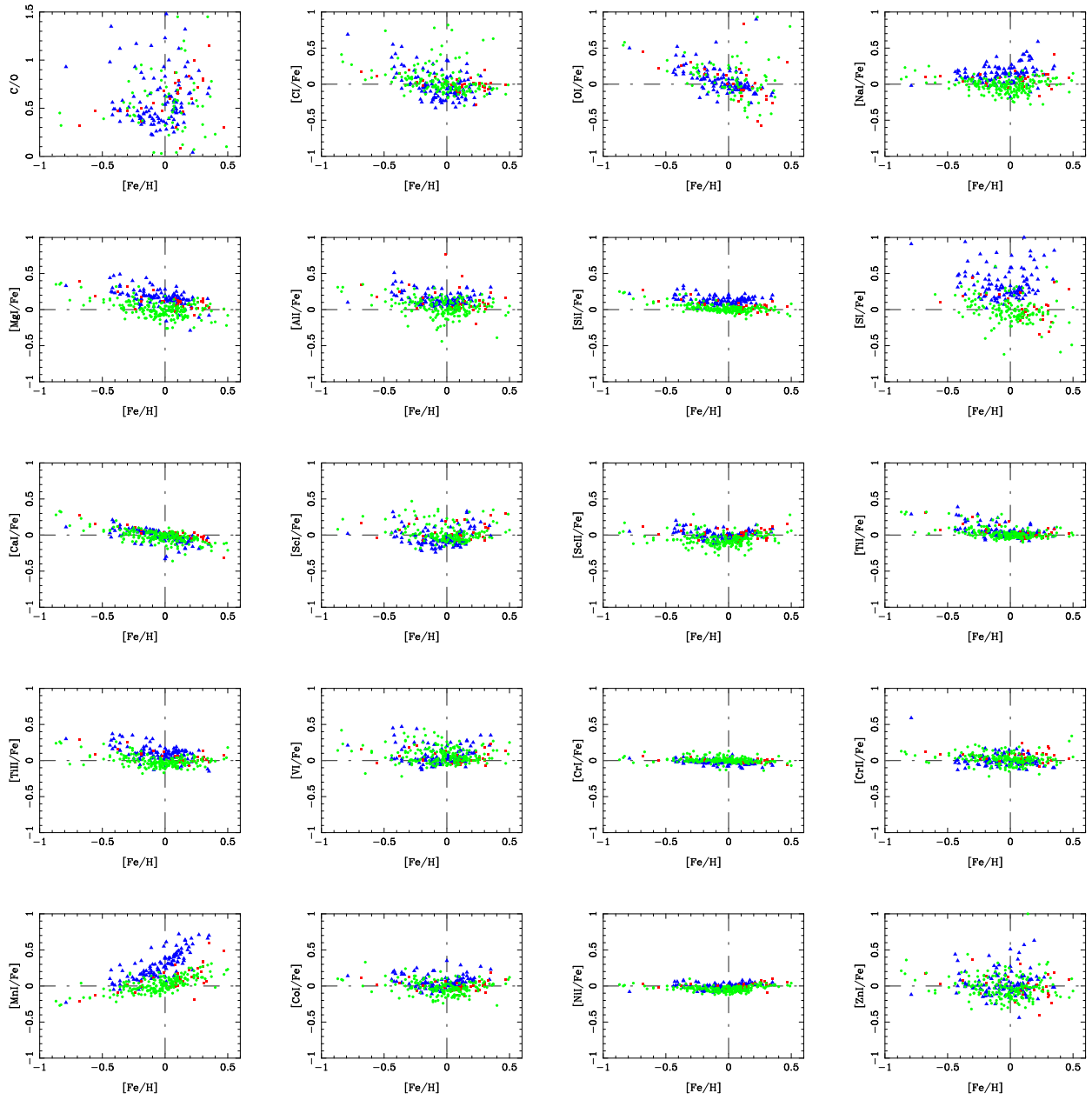


**Fig. A.1.** C/O and chemical abundance ratios of  $[X/Fe]$  as a function of the stellar metallicity. MS stars are plotted as green circles, subgiants as red squares, and giants as blue triangles.

**Online material**

Table 2 gives the abundances of C I, O I, Na I, Mg I, Al I, Si I, S I, Ca I, Sc I, Sc II, Ti I, Ti II, V I (HFS taken into account), Cr I, Cr II Mn I, Co I (HFS taken into account), Ni I, and Zn I. They are expressed relative to the solar value, i.e.  $[X/H] = \log(N_X/N_H) - \log(N_X/N_H)_\odot$ . For each star abundances are given in the first row, whilst uncertainties are given in the second row. Note that the data for the majority of the main-sequence stars comes from MA15 and is not reproduced here. Abundances of carbon and oxygen of the stars from M15 were recomputed as described in Section 2. They are given in Table 3.

Results produced in the framework of this work are only available in the electronic version of the corresponding paper or at the CDS via anonymous ftp to [cdsarc.u-strasbg.fr](ftp://cdsarc.u-strasbg.fr) (130.79.128.5) or via <http://cdsweb.u-strasbg.fr/cgi-bin/qcat?J/A+A/>

Table 1 lists all the stars analysed in this work. Note that the data for the majority of the main-sequence stars comes from MA15 and is not reproduced here. The table provides: HIP number (column 1); HD number (column 2); effective temperature in kelvin (column 3); logarithm of the surface gravity in  $\text{cms}^{-2}$  (column 4); microturbulent velocity in  $\text{kms}^{-1}$  (column 5); final metallicity in dex (column 6); spectrograph (column 7); stellar age in Gyr (column 8); stellar mass in solar units (column 9); and stellar radii in solar units (column 10). Each measured quantity is accompanied by its corresponding uncertainty.



**Table 1.** Spectroscopic parameters with uncertainties for the stars measured in this work.

HIP	HD	$T_{\text{eff}}$ (K)	$\log g$ ( $\text{cms}^{-2}$ )	$\xi_r$ ( $\text{kms}^{-1}$ )	[Fe/H] dex	Sp. <sup>†</sup>	Age (Gyr)	$M_{\star}$ ( $M_{\odot}$ )	$R_{\star}$ ( $R_{\odot}$ )
(1)	(2)	(3)	(4)	(5)	(6)	(7)	(8)	(9)	(10)
Giant stars with planets									
1692	1690	4338 ± 20	2.04 ± 0.08	1.56 ± 0.14	-0.24 ± 0.04	3	6.80 ± 3.12	1.11 ± 0.15	18.60 ± 2.72
4297	5319	4895 ± 28	3.33 ± 0.09	1.10 ± 0.10	0.05 ± 0.03	3	4.48 ± 0.85	1.30 ± 0.07	3.76 ± 0.35
10085	13189	4187 ± 35	1.60 ± 0.14	1.49 ± 0.17	-0.36 ± 0.06	4	4.41 ± 2.89	1.24 ± 0.27	32.32 ± 6.08
12247	16400	4864 ± 23	2.65 ± 0.08	1.41 ± 0.10	-0.03 ± 0.03	3	1.68 ± 0.18	1.83 ± 0.09	9.79 ± 0.36
20889	28305	4911 ± 25	2.73 ± 0.09	1.39 ± 0.13	0.15 ± 0.04	4	0.63 ± 0.07	2.63 ± 0.07	12.45 ± 0.26
36616	59686	4669 ± 20	2.63 ± 0.07	1.32 ± 0.11	0.13 ± 0.04	4	1.48 ± 0.46	1.98 ± 0.19	12.57 ± 0.44
37826	62509	4887 ± 18	3.00 ± 0.06	1.23 ± 0.10	0.09 ± 0.03	4	1.31 ± 0.17	2.03 ± 0.07	8.63 ± 0.16
42527	73108	4517 ± 18	2.39 ± 0.08	1.30 ± 0.10	-0.17 ± 0.03	4	10.10 ± 1.17	1.01 ± 0.04	9.72 ± 0.29
46471	81688	4773 ± 13	2.38 ± 0.05	1.41 ± 0.08	-0.36 ± 0.02	4	3.39 ± 1.90	1.33 ± 0.22	10.60 ± 0.38
50887	90043	4999 ± 10	3.25 ± 0.04	1.11 ± 0.06	-0.09 ± 0.02	4	3.87 ± 0.29	1.31 ± 0.03	3.39 ± 0.11
53666	95089	4936 ± 15	3.31 ± 0.05	1.08 ± 0.08	0.00 ± 0.02	4	2.95 ± 0.54	1.48 ± 0.09	4.52 ± 0.53
57428	102272	4814 ± 18	2.64 ± 0.06	1.45 ± 0.12	-0.41 ± 0.03	4	7.12 ± 2.85	1.05 ± 0.12	7.10 ± 1.16
57820	102956	4978 ± 30	3.40 ± 0.10	1.13 ± 0.13	0.14 ± 0.04	3	2.68 ± 0.47	1.56 ± 0.09	4.06 ± 0.44
58952	104985	4685 ± 15	2.43 ± 0.06	1.37 ± 0.09	-0.36 ± 0.02	4	4.39 ± 0.54	1.22 ± 0.05	10.64 ± 0.29
61740	110014	4605 ± 40	2.53 ± 0.14	1.37 ± 0.18	0.35 ± 0.06	4	0.46 ± 0.07	2.94 ± 0.10	17.62 ± 0.69
74793	136726	4260 ± 33	1.94 ± 0.13	1.43 ± 0.16	0.00 ± 0.06	4	2.08 ± 0.65	1.69 ± 0.18	26.63 ± 1.03
74961	136418	4985 ± 10	3.41 ± 0.05	1.02 ± 0.08	-0.11 ± 0.02	4	4.32 ± 0.51	1.27 ± 0.05	3.42 ± 0.19
75458	137759	4582 ± 30	2.72 ± 0.10	1.19 ± 0.12	0.19 ± 0.05	4	3.60 ± 0.98	1.46 ± 0.14	11.51 ± 0.29
76311	139357	4601 ± 28	2.63 ± 0.10	1.25 ± 0.14	0.34 ± 0.05	4	1.19 ± 0.33	2.16 ± 0.18	12.53 ± 0.56
77655	142091	4865 ± 15	3.30 ± 0.05	1.06 ± 0.08	0.09 ± 0.02	4	3.23 ± 0.15	1.46 ± 0.03	4.79 ± 0.04
79219	145457	4797 ± 20	2.53 ± 0.06	1.36 ± 0.08	-0.20 ± 0.03	4	4.80 ± 3.16	1.24 ± 0.24	9.67 ± 0.82
80687	148427	5017 ± 20	3.51 ± 0.06	1.09 ± 0.10	0.06 ± 0.03	3	3.44 ± 0.16	1.40 ± 0.03	3.19 ± 0.13
88048	163917	4965 ± 20	2.88 ± 0.08	1.51 ± 0.13	0.15 ± 0.04	3	0.38 ± 0.01	3.04 ± 0.05	13.30 ± 0.27
89047	167042	4983 ± 10	3.53 ± 0.04	1.10 ± 0.08	0.03 ± 0.02	3	2.69 ± 0.09	1.53 ± 0.02	4.26 ± 0.10
90344	170693	4515 ± 15	2.40 ± 0.07	1.39 ± 0.09	-0.34 ± 0.03	3	3.13 ± 1.51	1.37 ± 0.21	18.83 ± 0.52
91852	173416	4775 ± 30	2.35 ± 0.10	1.37 ± 0.12	-0.12 ± 0.04	3	1.62 ± 0.60	1.83 ± 0.24	12.50 ± 0.63
92895	175541	5052 ± 35	3.37 ± 0.11	1.07 ± 0.15	-0.07 ± 0.04	3	3.14 ± 0.62	1.42 ± 0.10	3.68 ± 0.48
94576	180314	4990 ± 30	3.04 ± 0.10	1.27 ± 0.15	0.22 ± 0.04	3	0.75 ± 0.06	2.41 ± 0.07	8.16 ± 0.46
94951	180902	5026 ± 15	3.54 ± 0.05	1.11 ± 0.10	0.01 ± 0.03	3	2.87 ± 0.37	1.49 ± 0.07	3.76 ± 0.36
95124	181342	4998 ± 15	3.42 ± 0.05	1.13 ± 0.11	0.20 ± 0.03	3	2.07 ± 0.24	1.71 ± 0.07	4.41 ± 0.30
97938	188310	4796 ± 30	2.66 ± 0.10	1.44 ± 0.15	-0.15 ± 0.04	3	3.16 ± 2.50	1.43 ± 0.34	9.71 ± 0.34
99894	192699	5101 ± 25	3.24 ± 0.08	1.08 ± 0.11	-0.19 ± 0.03	3	2.59 ± 0.21	1.48 ± 0.05	4.20 ± 0.18
103527	199665	5106 ± 30	3.10 ± 0.09	1.34 ± 0.13	0.07 ± 0.04	3	0.84 ± 0.03	2.28 ± 0.04	7.32 ± 0.23
104202	200964	5067 ± 20	3.30 ± 0.07	1.04 ± 0.11	-0.11 ± 0.03	3	2.50 ± 0.20	1.53 ± 0.05	4.28 ± 0.18
107251	206610	4953 ± 45	3.43 ± 0.14	1.01 ± 0.20	0.22 ± 0.06	3	1.97 ± 0.70	1.74 ± 0.21	5.07 ± 1.19
109577	210702	4993 ± 15	3.42 ± 0.05	1.14 ± 0.08	0.02 ± 0.02	3	2.24 ± 0.12	1.63 ± 0.03	4.71 ± 0.13
110813	212771	5018 ± 15	3.36 ± 0.06	1.09 ± 0.08	-0.17 ± 0.02	3	2.58 ± 0.49	1.49 ± 0.10	4.84 ± 0.56
114855	219449	4686 ± 20	2.57 ± 0.08	1.41 ± 0.12	0.00 ± 0.04	3	6.34 ± 1.99	1.19 ± 0.12	10.70 ± 0.25
116076	221345	4773 ± 10	2.68 ± 0.04	1.45 ± 0.10	-0.26 ± 0.02	3	7.26 ± 2.14	1.08 ± 0.09	10.69 ± 0.26
	17092	4630 ± 30	2.47 ± 0.11	1.32 ± 0.13	0.11 ± 0.05	4	5.82 ± 2.75	1.23 ± 0.18	7.72 ± 2.83
BD+20 2457		4257 ± 20	1.63 ± 0.08	1.62 ± 0.09	-0.79 ± 0.03	3	4.55 ± 4.06		
$\gamma$ 1 Leo		4376 ± 15	1.67 ± 0.06	1.43 ± 0.10	-0.44 ± 0.03	4	1.94 ± 0.46	1.59 ± 0.12	30.09 ± 1.08
	240210	4309 ± 33	1.83 ± 0.14	1.49 ± 0.16	-0.11 ± 0.06	3	7.90 ± 2.81	1.10 ± 0.11	16.12 ± 2.25
Giant stars without planets									
729	448	4811 ± 23	2.69 ± 0.09	1.40 ± 0.12	0.04 ± 0.04	3	1.77 ± 0.19	1.81 ± 0.08	9.91 ± 0.32
873	645	4849 ± 15	3.08 ± 0.05	1.19 ± 0.08	0.03 ± 0.02	3	1.72 ± 0.14	1.78 ± 0.05	7.30 ± 0.23
6682	8594	4833 ± 15	3.17 ± 0.05	1.14 ± 0.09	0.00 ± 0.03	3	4.28 ± 0.71	1.31 ± 0.07	4.91 ± 0.31
6999	9057	4961 ± 20	2.87 ± 0.08	1.44 ± 0.11	0.07 ± 0.03	3	0.76 ± 0.09	2.43 ± 0.08	10.78 ± 0.33
7097	9270	4936 ± 40	2.18 ± 0.14	1.73 ± 0.24	-0.09 ± 0.06	3	0.24 ± 0.03	3.62 ± 0.14	27.01 ± 2.26
7607	9927	4396 ± 38	2.17 ± 0.14	1.46 ± 0.16	0.11 ± 0.07	3	1.78 ± 0.49	1.85 ± 0.20	20.54 ± 0.74
7719	10072	5097 ± 20	2.70 ± 0.06	1.31 ± 0.07	-0.12 ± 0.02	3	0.77 ± 0.11	2.32 ± 0.10	9.68 ± 0.41
9222	11949	4803 ± 10	2.94 ± 0.04	1.21 ± 0.08	-0.15 ± 0.02	3	2.51 ± 0.20	1.52 ± 0.04	8.00 ± 0.21
13531	17878	5025 ± 25	2.48 ± 0.09	1.19 ± 0.11	-0.20 ± 0.03	3	0.43 ± 0.04	2.91 ± 0.08	16.43 ± 0.55
19038	25604	4808 ± 28	2.74 ± 0.09	1.39 ± 0.12	0.09 ± 0.04	3	1.09 ± 0.21	2.24 ± 0.12	11.20 ± 0.28
42528	73764	5128 ± 20	3.36 ± 0.07	1.21 ± 0.12	0.01 ± 0.03	3	1.75 ± 0.13	1.76 ± 0.05	4.60 ± 0.21
59285	105639	4637 ± 33	2.82 ± 0.13	1.22 ± 0.14	0.09 ± 0.05	3	4.14 ± 0.77	1.35 ± 0.08	7.85 ± 0.28

Table 1. Continued.

HIP	HD	T <sub>eff</sub> (K)	log g (c <sub>ms</sub> <sup>-2</sup> )	ξ <sub>t</sub> (k <sub>ms</sub> <sup>-1</sup> )	[Fe/H] dex	Sp. <sup>†</sup>	Age (Gyr)	M <sub>★</sub> (M <sub>☉</sub> )	R <sub>★</sub> (R <sub>☉</sub> )
(1)	(2)	(3)	(4)	(5)	(6)	(7)	(8)	(9)	(10)
59646	106314	5132 ± 23	3.61 ± 0.06	1.13 ± 0.12	0.10 ± 0.03	3	2.87 ± 0.14	1.52 ± 0.03	3.33 ± 0.11
59847	106714	4872 ± 20	2.46 ± 0.08	1.41 ± 0.10	-0.20 ± 0.03	3	2.16 ± 0.44	1.61 ± 0.12	10.97 ± 0.28
59856	106760	4581 ± 28	2.48 ± 0.10	1.39 ± 0.16	-0.12 ± 0.05	3	1.57 ± 0.32	1.85 ± 0.14	16.79 ± 0.79
68904	123351	4883 ± 23	3.44 ± 0.08	1.56 ± 0.14	0.03 ± 0.03	3	4.24 ± 0.67	1.32 ± 0.06	4.11 ± 0.27
69185	123929	5066 ± 13	3.36 ± 0.04	1.06 ± 0.06	-0.29 ± 0.02	3	3.57 ± 0.37	1.29 ± 0.05	3.89 ± 0.20
69427	124294	4235 ± 20	1.83 ± 0.08	1.48 ± 0.11	-0.43 ± 0.04	3	8.55 ± 1.57	1.00 ± 0.06	25.43 ± 0.73
69612	124679	4809 ± 23	2.71 ± 0.08	1.38 ± 0.11	-0.08 ± 0.03	3	2.29 ± 0.44	1.61 ± 0.11	10.56 ± 0.32
70027	125560	4556 ± 48	2.54 ± 0.17	1.37 ± 0.19	0.27 ± 0.07	3	5.50 ± 2.80	1.29 ± 0.20	11.06 ± 0.37
70038	125490	5071 ± 23	3.00 ± 0.07	1.20 ± 0.09	-0.04 ± 0.03	3	1.11 ± 0.10	2.04 ± 0.07	6.60 ± 0.34
80816	148856	5000 ± 20	2.40 ± 0.07	1.52 ± 0.11	-0.10 ± 0.03	3	0.45 ± 0.04	2.89 ± 0.07	15.55 ± 0.46
84975	157261	5000 ± 20	3.33 ± 0.06	1.16 ± 0.08	-0.17 ± 0.02	3	2.99 ± 0.28	1.42 ± 0.05	4.67 ± 0.22
88765	165760	4998 ± 15	2.70 ± 0.05	1.48 ± 0.10	-0.01 ± 0.03	3	0.56 ± 0.06	2.68 ± 0.07	12.96 ± 0.36
88836	166229	4647 ± 33	2.82 ± 0.13	1.24 ± 0.16	0.21 ± 0.06	3	2.96 ± 0.56	1.52 ± 0.10	8.43 ± 0.26
89826	168775	4639 ± 28	2.52 ± 0.10	1.49 ± 0.16	0.13 ± 0.05	3	0.66 ± 0.17	2.62 ± 0.18	17.27 ± 0.48
89918	168656	5061 ± 18	2.80 ± 0.06	1.39 ± 0.08	-0.09 ± 0.02	3	0.69 ± 0.08	2.45 ± 0.07	10.97 ± 0.32
89962	168723	4948 ± 15	3.18 ± 0.05	1.19 ± 0.08	-0.19 ± 0.02	3	2.76 ± 0.18	1.45 ± 0.04	5.72 ± 0.09
95822	183492	4819 ± 25	2.71 ± 0.08	1.36 ± 0.10	0.07 ± 0.03	3	1.61 ± 0.29	1.92 ± 0.14	10.14 ± 0.38
95926	183756	4999 ± 15	3.60 ± 0.05	1.04 ± 0.08	-0.06 ± 0.02	3	3.73 ± 0.32	1.33 ± 0.04	3.36 ± 0.14
96016	184010	4997 ± 13	3.24 ± 0.05	1.12 ± 0.06	-0.13 ± 0.02	3	2.27 ± 0.15	1.57 ± 0.04	5.27 ± 0.15
96229	184406	4535 ± 33	2.83 ± 0.12	1.14 ± 0.16	0.16 ± 0.06	3	7.72 ± 1.96	1.14 ± 0.08	7.58 ± 0.22
98210	188844	4819 ± 18	3.04 ± 0.06	1.18 ± 0.09	-0.17 ± 0.03	3	3.84 ± 0.60	1.31 ± 0.07	6.56 ± 0.32
98314	189186	5021 ± 10	3.14 ± 0.04	1.18 ± 0.07	-0.36 ± 0.02	3	3.44 ± 0.41	1.30 ± 0.05	4.96 ± 0.25
98845	190571	5086 ± 30	3.15 ± 0.09	1.07 ± 0.14	-0.25 ± 0.04	3	3.85 ± 0.56	1.27 ± 0.06	3.50 ± 0.19
98920	190608	4775 ± 28	3.00 ± 0.10	1.16 ± 0.13	0.09 ± 0.04	3	2.43 ± 0.33	1.60 ± 0.08	7.11 ± 0.21
99171	191067	4779 ± 20	3.28 ± 0.07	1.06 ± 0.09	-0.04 ± 0.03	3	8.67 ± 1.27	1.07 ± 0.05	4.51 ± 0.13
99841	192787	5024 ± 15	2.97 ± 0.05	1.33 ± 0.08	-0.11 ± 0.02	3	1.00 ± 0.15	2.16 ± 0.09	9.15 ± 0.29
99913	192836	4805 ± 15	2.89 ± 0.05	1.24 ± 0.10	0.07 ± 0.03	3	1.62 ± 0.14	1.87 ± 0.05	9.29 ± 0.42
100022	193343	4936 ± 28	3.57 ± 0.09	1.05 ± 0.12	0.18 ± 0.04	3	3.63 ± 0.31	1.42 ± 0.05	3.50 ± 0.16
100503	194110	5114 ± 10	3.48 ± 0.03	1.08 ± 0.06	-0.22 ± 0.01	3	2.99 ± 0.15	1.39 ± 0.03	3.67 ± 0.18
100541	194013	4932 ± 20	2.91 ± 0.06	1.40 ± 0.09	-0.06 ± 0.03	3	1.44 ± 0.23	1.95 ± 0.10	8.93 ± 0.30
100587	194317	4263 ± 35	2.02 ± 0.14	1.42 ± 0.16	0.01 ± 0.06	3	4.64 ± 2.01	1.31 ± 0.18	21.80 ± 0.82
101848	196645	5066 ± 20	3.41 ± 0.06	1.06 ± 0.08	-0.17 ± 0.02	3	3.97 ± 0.51	1.28 ± 0.05	3.18 ± 0.22
101936	196758	4796 ± 33	2.72 ± 0.11	1.39 ± 0.14	0.07 ± 0.05	3	1.76 ± 0.31	1.83 ± 0.13	9.94 ± 0.46
102532	197964	4801 ± 18	3.05 ± 0.06	1.22 ± 0.09	0.13 ± 0.03	3	1.48 ± 0.12	1.94 ± 0.05	8.42 ± 0.29
103004	198809	5261 ± 15	2.97 ± 0.05	1.38 ± 0.10	-0.05 ± 0.02	3	0.70 ± 0.04	2.40 ± 0.05	8.01 ± 0.30
103519	199870	4993 ± 20	3.11 ± 0.06	1.27 ± 0.11	0.12 ± 0.03	3	0.80 ± 0.04	2.33 ± 0.05	8.07 ± 0.24
105390	203358	5066 ± 18	3.45 ± 0.06	1.05 ± 0.08	-0.23 ± 0.02	3	2.95 ± 0.21	1.40 ± 0.04	4.22 ± 0.19
105411	203344	4809 ± 25	2.77 ± 0.08	1.42 ± 0.12	-0.10 ± 0.03	3	1.65 ± 0.43	1.77 ± 0.15	9.39 ± 0.34
105502	203504	4673 ± 20	2.59 ± 0.06	1.42 ± 0.11	0.00 ± 0.03	3	3.22 ± 0.72	1.47 ± 0.11	11.59 ± 0.23
106081	204642	4716 ± 28	3.03 ± 0.09	1.14 ± 0.11	0.11 ± 0.04	3	3.64 ± 0.66	1.41 ± 0.09	6.71 ± 0.42
106093	204771	4953 ± 15	3.01 ± 0.05	1.33 ± 0.10	0.06 ± 0.03	3	1.26 ± 0.16	2.02 ± 0.07	8.30 ± 0.15
110538	212496	4727 ± 13	2.64 ± 0.05	1.26 ± 0.08	-0.30 ± 0.02	3	3.01 ± 0.85	1.39 ± 0.11	10.49 ± 0.11
111944	214868	4352 ± 25	1.93 ± 0.10	1.54 ± 0.15	-0.19 ± 0.05	3	1.97 ± 0.57	1.66 ± 0.16	26.03 ± 0.94
112041	215030	4788 ± 13	2.65 ± 0.05	1.26 ± 0.08	-0.42 ± 0.02	3	4.31 ± 0.64	1.21 ± 0.06	8.89 ± 0.33
112067	214995	4713 ± 28	2.63 ± 0.10	1.40 ± 0.16	-0.01 ± 0.05	3	2.85 ± 0.44	1.49 ± 0.09	8.75 ± 0.33
112158	215182	4986 ± 20	2.16 ± 0.06	1.57 ± 0.11	-0.21 ± 0.03	3	0.30 ± 0.03	3.30 ± 0.09	22.27 ± 1.11
112242	215373	5035 ± 20	2.90 ± 0.06	1.45 ± 0.12	0.10 ± 0.03	3	0.59 ± 0.02	2.59 ± 0.04	9.57 ± 0.24
115696	220807	4887 ± 10	3.05 ± 0.04	1.20 ± 0.06	-0.40 ± 0.02	3	8.03 ± 1.12	1.02 ± 0.04	5.49 ± 0.24
115830	220954	4756 ± 25	2.67 ± 0.09	1.36 ± 0.12	0.08 ± 0.04	3	1.72 ± 0.13	1.83 ± 0.05	9.63 ± 0.22
115919	221115	5034 ± 15	2.93 ± 0.05	1.37 ± 0.10	0.05 ± 0.03	3	0.74 ± 0.05	2.39 ± 0.06	8.44 ± 0.38
116584	222107	4888 ± 30	3.22 ± 0.10	1.40 ± 0.16	-0.42 ± 0.04	3	5.62 ± 1.28	1.12 ± 0.08	6.41 ± 0.15
116823	222455	4554 ± 38	2.78 ± 0.14	1.18 ± 0.15	0.16 ± 0.06	3	9.28 ± 1.87	1.09 ± 0.06	6.05 ± 0.60
117375	223252	5010 ± 25	2.84 ± 0.09	1.40 ± 0.10	-0.05 ± 0.03	3	0.85 ± 0.12	2.32 ± 0.09	10.17 ± 0.31
117411	223301	4745 ± 25	3.22 ± 0.09	1.11 ± 0.12	0.17 ± 0.04	3	6.34 ± 1.43	1.20 ± 0.08	4.40 ± 0.31
117541	223524	4656 ± 30	2.58 ± 0.11	1.36 ± 0.13	0.10 ± 0.05	3	4.91 ± 3.37	1.30 ± 0.27	10.22 ± 0.55
Subgiant stars with planets									
8159	10697	5631 ± 15	3.99 ± 0.04	1.16 ± 0.10	0.10 ± 0.02	3	7.61 ± 0.20	1.10 ± 0.01	1.73 ± 0.03
12048	16141	5759 ± 15	4.10 ± 0.04	1.15 ± 0.09	0.11 ± 0.02	3	7.49 ± 0.25	1.09 ± 0.01	1.55 ± 0.05
12191	16175	5958 ± 18	4.12 ± 0.04	1.26 ± 0.11	0.26 ± 0.02	4	3.51 ± 0.34	1.31 ± 0.03	1.68 ± 0.07

**Table 1.** Continued.

HIP	HD	T <sub>eff</sub> (K)	log g (cms <sup>-2</sup> )	ξ <sub>t</sub> (kms <sup>-1</sup> )	[Fe/H] dex	Sp. <sup>†</sup>	Age (Gyr)	M <sub>★</sub> (M <sub>☉</sub> )	R <sub>★</sub> (R <sub>☉</sub> )
(1)	(2)	(3)	(4)	(5)	(6)	(7)	(8)	(9)	(10)
27253	38529	5585 ± 18	3.86 ± 0.05	1.19 ± 0.09	0.30 ± 0.02	4	3.83 ± 0.07	1.38 ± 0.01	2.49 ± 0.04
36795	60532	6092 ± 28	3.50 ± 0.05	1.72 ± 0.15	-0.24 ± 0.02	4	3.02 ± 0.01	1.36 ± 0.01	2.64 ± 0.03
42446	73534	5016 ± 43	3.84 ± 0.13	0.89 ± 0.25	0.30 ± 0.06	3	5.53 ± 0.82	1.24 ± 0.05	2.33 ± 0.15
49813	88133	5426 ± 13	3.98 ± 0.04	1.03 ± 0.09	0.30 ± 0.02	4	5.44 ± 0.79	1.24 ± 0.05	2.05 ± 0.15
54195	96167	5769 ± 15	4.07 ± 0.04	1.23 ± 0.09	0.29 ± 0.02	4	4.24 ± 0.61	1.30 ± 0.07	1.83 ± 0.14
66192	118203	5807 ± 20	3.95 ± 0.05	1.22 ± 0.11	0.19 ± 0.02	4	4.32 ± 0.64	1.30 ± 0.07	1.90 ± 0.13
93746	177830	4878 ± 40	3.73 ± 0.13	0.96 ± 0.22	0.47 ± 0.06	3	4.28 ± 0.36	1.35 ± 0.04	3.08 ± 0.14
94256	179079	5777 ± 33	4.20 ± 0.08	1.22 ± 0.18	0.33 ± 0.04	3	4.89 ± 0.79	1.20 ± 0.04	1.50 ± 0.08
96507	185269	6053 ± 40	4.04 ± 0.09	1.50 ± 0.21	0.14 ± 0.04	3	3.40 ± 0.44	1.35 ± 0.05	1.88 ± 0.06
100970	195019	5777 ± 25	4.09 ± 0.05	1.09 ± 0.14	0.09 ± 0.03	3	7.86 ± 0.43	1.07 ± 0.02	1.43 ± 0.06
114699	219077	5291 ± 8	3.91 ± 0.02	0.98 ± 0.03	-0.19 ± 0.01	8	8.63 ± 0.25	1.03 ± 0.01	1.99 ± 0.03
115100	219828	5838 ± 13	4.13 ± 0.03	1.26 ± 0.10	0.12 ± 0.02	3	6.36 ± 0.75	1.13 ± 0.04	1.55 ± 0.09
118319	224693	5983 ± 25	4.21 ± 0.05	1.37 ± 0.14	0.21 ± 0.02	3	3.51 ± 0.45	1.34 ± 0.06	1.79 ± 0.16
HAT-P-7		6563 ± 40	4.05 ± 0.06	1.86 ± 0.21	0.23 ± 0.03	3	1.01 ± 0.63	1.49 ± 0.14	1.71 ± 0.43
Subgiant stars without planets									
6512	8375	5244 ± 10	3.72 ± 0.04	1.10 ± 0.06	-0.09 ± 0.01	3	2.40 ± 0.09	1.55 ± 0.02	3.62 ± 0.10
12350	16548	5642 ± 10	3.94 ± 0.03	1.17 ± 0.05	0.10 ± 0.01	8	5.63 ± 0.50	1.19 ± 0.03	1.96 ± 0.06
14086	18907	5021 ± 10	3.60 ± 0.03	0.93 ± 0.05	-0.68 ± 0.01	8			
15776	21019	5346 ± 10	3.66 ± 0.02	1.09 ± 0.06	-0.56 ± 0.01	8	7.17 ± 0.36	1.01 ± 0.02	2.36 ± 0.06
17183	22918	4896 ± 13	3.68 ± 0.04	0.87 ± 0.09	-0.01 ± 0.02	8	8.60 ± 0.77	1.07 ± 0.03	2.73 ± 0.09
17378	23249	5057 ± 15	3.80 ± 0.04	0.96 ± 0.08	0.08 ± 0.02	8	6.30 ± 0.18	1.17 ± 0.01	2.29 ± 0.02
18432	24892	5306 ± 8	3.90 ± 0.03	0.97 ± 0.04	-0.38 ± 0.01	8	10.60 ± 0.55	0.93 ± 0.02	1.92 ± 0.05
60585	108103	5792 ± 43	4.23 ± 0.12	0.97 ± 0.22	0.31 ± 0.04	3	3.69 ± 1.84	1.13 ± 0.03	1.20 ± 0.10
64408	114613	5672 ± 10	3.95 ± 0.02	1.20 ± 0.05	0.12 ± 0.01	8	4.76 ± 0.07	1.26 ± 0.01	2.09 ± 0.01
70616	126647	4999 ± 43	3.89 ± 0.13	0.99 ± 0.23	0.35 ± 0.06	3	4.14 ± 0.21	1.36 ± 0.03	2.73 ± 0.13
81819	150474	5404 ± 10	4.01 ± 0.02	1.04 ± 0.04	-0.02 ± 0.01	8	7.81 ± 0.76	1.09 ± 0.03	1.92 ± 0.08
98036	188512	5117 ± 10	3.64 ± 0.03	1.01 ± 0.05	-0.19 ± 0.01	8	3.56 ± 0.09	1.32 ± 0.01	3.04 ± 0.05
98138	188993	5838 ± 28	3.62 ± 0.06	1.61 ± 0.12	0.04 ± 0.03	3	2.26 ± 0.23	1.62 ± 0.06	3.51 ± 0.25
102531	197963	6297 ± 28	3.77 ± 0.05	1.58 ± 0.10	0.08 ± 0.02	3	2.01 ± 0.09	1.62 ± 0.03	2.60 ± 0.12
109822	211038	4956 ± 5	3.70 ± 0.02	0.88 ± 0.05	-0.30 ± 0.01	8	11.48 ± 0.01	0.93 ± 0.00	2.69 ± 0.06
116250	221420	5793 ± 10	4.03 ± 0.03	1.28 ± 0.05	0.26 ± 0.01	8	3.93 ± 0.38	1.34 ± 0.04	1.92 ± 0.03
Main-sequence stars with planets									
20723	28185	5665 ± 13	4.51 ± 0.03	0.92 ± 0.09	0.21 ± 0.01	4	6.03 ± 1.17	1.03 ± 0.01	1.09 ± 0.04
31246	46375	5313 ± 18	4.68 ± 0.05	0.70 ± 0.23	0.30 ± 0.03	4	9.99 ± 1.43	0.92 ± 0.01	0.98 ± 0.03
60081	107148	5788 ± 13	4.47 ± 0.03	1.03 ± 0.07	0.26 ± 0.01	4	4.09 ± 0.98	1.10 ± 0.01	1.14 ± 0.05
80838	149026	6299 ± 30	4.72 ± 0.05	1.32 ± 0.24	0.49 ± 0.04	3	0.55 ± 0.34	1.36 ± 0.02	1.38 ± 0.06
95740	183263	6041 ± 40	4.53 ± 0.08	1.00 ± 0.20	0.47 ± 0.04	3	0.74 ± 0.53	1.24 ± 0.02	1.22 ± 0.04
98767	190360	5621 ± 25	4.45 ± 0.06	1.02 ± 0.10	0.23 ± 0.02	3	7.05 ± 0.83	1.02 ± 0.01	1.10 ± 0.01
109378	210277	5593 ± 18	4.50 ± 0.04	0.96 ± 0.11	0.23 ± 0.02	3	4.13 ± 1.09	1.02 ± 0.01	0.99 ± 0.02
113357	217014	5811 ± 15	4.40 ± 0.04	1.13 ± 0.06	0.18 ± 0.01	3	4.27 ± 0.46	1.08 ± 0.01	1.10 ± 0.01
113421	217107	5679 ± 20	4.47 ± 0.05	1.03 ± 0.10	0.36 ± 0.02	3	3.98 ± 0.65	1.07 ± 0.01	1.09 ± 0.01
GSC02883-01687		5644 ± 28	4.38 ± 0.08	0.93 ± 0.19	0.32 ± 0.03	3	0.45 ± 0.31	1.05 ± 0.01	0.94 ± 0.02
TrES-4		6595 ± 75	4.47 ± 0.13	2.05 ± 0.37	0.40 ± 0.05	3	0.56 ± 0.34	1.48 ± 0.03	1.54 ± 0.07

**Notes.** <sup>†</sup>Spectrograph: (1) CAHA/FOCES; (2) TNG/SARG; (3) NOT/FIES; (4) MERCATOR/HERMES; (5) S<sup>4</sup>N-McD; (6) S<sup>4</sup>N-FEROS; (7) ESO/FEROS; (8) ESO/HARPS

**Table 2.** Derived abundances [X/H]

Star	C I	O I	Na I	Mg I	Al I	Si I	S I	Ca I	Sc I	Sc II	Ti I	Ti II	V I	Cr I	Cr II	Mn I	Co I	Ni I	Zn I
Giant stars with planets																			
HIP1692	0.13	-0.06	-0.15	-0.09	0.06	-0.03	0.53	-0.36	-0.01	-0.15	-0.04	-0.14	0.20	-0.27	-0.18	0.07	0.01	-0.19	-0.28
	0.05	0.03	0.09	0.05	0.04	0.06	0.22	0.14	0.33	0.06	0.09	0.11	0.13	0.07	0.08	0.09	0.09	0.04	0.23
HIP4297	0.02	0.02	0.13	0.17	0.20	0.12	0.30	0.01	0.04	0.01	0.04	0.07	0.09	0.02	0.02	0.37	0.08	0.06	0.06
	0.07	0.04	0.04	0.05	0.02	0.04	0.07	0.07	0.17	0.06	0.07	0.10	0.06	0.06	0.08	0.10	0.06	0.04	0.15
HIP10085	0.16	-0.10	-0.15	-0.02	-0.10	-0.03	0.58	-0.37	-0.18	-0.28	-0.18	-0.12	0.11	-0.31	-0.37	-0.07	-0.17	-0.28	-0.35
	0.08	0.03	0.07	0.05	0.09	0.07	0.05	0.12	0.46	0.06	0.08	0.13	0.10	0.06	0.09	0.11	0.07	0.04	0.05
HIP12247	-0.26	-0.04	0.11	0.20	0.07	0.09	0.20	-0.02	-0.13	-0.07	-0.02	0.04	-0.01	-0.04	-0.10	0.28	-0.02	-0.07	-0.03
	0.05	0.04	0.06	0.10	0.03	0.04	0.12	0.07	0.15	0.06	0.07	0.12	0.07	0.05	0.06	0.10	0.06	0.04	0.06
HIP20889	-0.05	0.10	0.48	0.30	0.24	0.29	0.45	0.12	0.02	0.12	0.07	0.23	0.06	0.10	0.17	0.53	0.14	0.12	0.11
	0.05	0.04	0.14	0.05	0.05	0.04	0.14	0.06	0.14	0.07	0.07	0.15	0.06	0.06	0.07	0.11	0.05	0.04	0.14
HIP36616	0.05	0.12	0.30	0.21	0.26	0.28	0.54	0.07	0.13	0.17	0.17	0.05	0.21	0.09	0.00	0.59	0.24	0.15	-0.01
	0.06	0.03	0.08	0.12	0.04	0.05	0.11	0.08	0.25	0.05	0.10	0.11	0.10	0.07	0.17	0.12	0.08	0.04	0.34
HIP37826	-0.11	0.01	0.24	0.23	0.16	0.20	0.34	0.06	-0.06	0.06	0.01	0.21	0.07	0.05	0.01	0.29	0.07	0.04	0.05
	0.05	0.04	0.06	0.06	0.02	0.04	0.10	0.06	0.16	0.06	0.07	0.13	0.07	0.05	0.12	0.10	0.06	0.04	0.12
HIP42527	-0.21	-0.07	0.07	0.08	0.05	-0.03	0.31	-0.15	-0.07	-0.10	-0.04	0.02	-0.01	-0.19	-0.21	0.04	-0.06	-0.17	0.25
	0.07	0.03	0.18	0.07	0.04	0.03	0.05	0.07	0.25	0.05	0.09	0.11	0.09	0.07	0.10	0.09	0.06	0.04	0.30
HIP46471	-0.31	-0.22	-0.28	-0.04	-0.13	-0.19	0.10	-0.27	-0.46	-0.34	-0.31	-0.22	-0.37	-0.40	-0.47	-0.29	-0.32	-0.38	-0.32
	0.06	0.03	0.09	0.07	0.04	0.03	0.06	0.08	0.13	0.04	0.10	0.08	0.12	0.07	0.13	0.09	0.06	0.03	0.07
HIP50887	-0.22	-0.34	-0.06	0.10	0.00	-0.01	0.18	-0.05	-0.16	-0.13	-0.05	-0.03	-0.08	-0.08	-0.13	0.03	-0.11	-0.13	-0.13
	0.10	0.04	0.04	0.09	0.03	0.03	0.15	0.07	0.10	0.06	0.06	0.08	0.06	0.05	0.08	0.09	0.05	0.04	0.06
HIP53666	-0.13	-0.07	0.01	0.19	0.10	0.10	0.20	0.03	-0.03	0.00	0.03	0.09	0.03	-0.02	-0.06	0.28	0.02	-0.02	-0.02
	0.05	0.03	0.04	0.07	0.03	0.03	0.10	0.06	0.14	0.05	0.05	0.08	0.05	0.04	0.12	0.10	0.04	0.04	0.07
HIP57428	0.01	0.11	-0.23	0.06	-0.02	-0.13	0.08	-0.23	-0.36	-0.27	-0.14	-0.11	-0.16	-0.43	-0.45	-0.46	-0.24	-0.35	-0.24
	0.06	0.03	0.06	0.09	0.07	0.02	0.06	0.07	0.14	0.05	0.10	0.11	0.12	0.07	0.08	0.09	0.07	0.03	0.08
HIP57820	0.19		0.13	0.28	0.22	0.24	0.48	0.08	0.05	0.10	0.12	0.28	0.13	0.12	0.25	0.45	0.13	0.17	0.18
	0.05		0.08	0.09	0.04	0.04	0.15	0.06	0.13	0.06	0.07	0.10	0.08	0.06	0.18	0.10	0.04	0.04	0.08
HIP58952	-0.09	0.03	-0.20	0.13	0.02	-0.07	0.16	-0.22	-0.33	-0.23	-0.14	-0.01	-0.21	-0.40	-0.38	-0.41	-0.20	-0.29	-0.16
	0.07	0.03	0.07	0.06	0.06	0.03	0.14	0.08	0.16	0.05	0.10	0.11	0.11	0.07	0.06	0.08	0.06	0.03	0.05
HIP61740	0.29	0.23	0.60	0.27	0.66	0.55	1.17	0.22	0.34	0.44	0.44	0.20	0.70	0.28	0.25	1.05	0.58	0.40	0.33
	0.07	0.03	0.05	0.06	0.10	0.06	0.09	0.07	0.37	0.07	0.10	0.14	0.14	0.07	0.11	0.18	0.08	0.04	0.52
HIP74793	0.33	0.02	0.13	0.18	0.18	0.21		-0.33	-0.04	0.01	0.06	-0.09	0.20	-0.04	-0.05	0.38	0.35	0.03	0.27
	0.03	0.03	0.08	0.04	0.03	0.05		0.26	0.43	0.06	0.06	0.17	0.03	0.05	0.09	0.14	0.24	0.04	0.05
HIP74961	-0.14	-0.06	0.00	0.07	0.03	-0.03	0.18	-0.09	-0.15	-0.13	-0.07	-0.08	-0.08	-0.12	-0.17	0.10	-0.09	-0.11	-0.10
	0.07	0.04	0.07	0.05	0.02	0.03	0.04	0.06	0.10	0.06	0.07	0.08	0.06	0.05	0.11	0.09	0.06	0.04	0.08
HIP75458	0.18	0.15	0.36	0.32	0.36	0.36	0.88	0.11	0.31	0.25	0.19	0.13	0.39	0.14	0.18	0.73	0.29	0.23	0.82
	0.05	0.03	0.07	0.06	0.04	0.05	0.05	0.08	0.30	0.07	0.10	0.12	0.10	0.07	0.08	0.13	0.06	0.04	0.30
HIP76311	0.21	0.18	0.55	0.49	0.51	0.49	0.76	0.30	0.47	0.38	0.32	0.22	0.55	0.30	0.24	1.00	0.43	0.36	0.32
	0.11	0.03	0.09	0.06	0.03	0.05	0.29	0.08	0.35	0.07	0.10	0.14	0.11	0.07	0.12	0.15	0.07	0.04	0.21
HIP77655	-0.03	0.01	0.18	0.25	0.25	0.20	0.34	0.06	0.12	0.10	0.09	0.14	0.15	0.07	0.04	0.51	0.13	0.12	0.03
	0.04	0.04	0.04	0.07	0.03	0.03	0.12	0.06	0.18	0.06	0.07	0.12	0.07	0.06	0.11	0.11	0.05	0.04	0.16
HIP79219	-0.15	-0.11	-0.09	0.06	-0.04	-0.05	0.04	-0.13	-0.32	-0.22	-0.14	-0.19	-0.18	-0.23	-0.28	-0.04	-0.17	-0.20	-0.30
	0.07	0.03	0.06	0.08	0.04	0.03	0.16	0.08	0.17	0.05	0.10	0.10	0.12	0.07	0.09	0.08	0.06	0.03	0.10
HIP80687	-0.06	0.24	0.16	0.25	0.17	0.14	0.32	0.02	-0.02	-0.03	0.08	0.17	0.11	0.07	0.03	0.35	0.09	0.08	0.10



Table 2. continued.

Star	C I	O I	Na I	Mg I	Al I	Si I	S I	Ca I	Sc I	Sc II	Ti I	Ti II	V I	Cr I	Cr II	Mn I	Co I	Ni I	Zn I
HIP88048	0.05	0.04	0.04	0.10	0.02	0.04	0.08	0.06	0.14	0.07	0.06	0.08	0.06	0.05	0.08	0.11	0.05	0.04	0.08
	-0.07	0.17	0.54	0.39	0.23	0.28	0.39	0.08	0.03	0.16	0.15	0.22	0.13	0.13	0.24	0.50	0.20	0.16	0.23
	0.05	0.04	0.10	0.05	0.04	0.04	0.06	0.07	0.15	0.07	0.07	0.13	0.06	0.05	0.18	0.09	0.06	0.04	0.06
HIP89047	-0.09	0.10	0.05	0.16	0.11	0.12	0.23	-0.02	-0.05	0.04	0.01	0.12	0.05	0.01	0.06	0.34	0.07	0.04	0.03
	0.05	0.04	0.05	0.05	0.02	0.03	0.07	0.06	0.14	0.06	0.07	0.09	0.06	0.05	0.07	0.10	0.06	0.04	0.07
HIP90344	-0.09	-0.06	-0.24	-0.11	-0.08	-0.14	0.33	-0.34	-0.22	-0.20	-0.14	-0.01	-0.15	-0.35	-0.39	-0.13	-0.18	-0.32	-0.32
	0.05	0.03	0.05	0.07	0.04	0.05	0.05	0.08	0.21	0.05	0.09	0.14	0.09	0.07	0.05	0.08	0.07	0.03	0.18
HIP91852	-0.12	-0.15	-0.05	0.25	-0.04	0.02	0.00	-0.08	-0.25	-0.18	-0.06	0.04	-0.08	-0.09	-0.12	0.15	-0.14	-0.17	-0.15
	0.08	0.03	0.05	0.14	0.05	0.05	0.10	0.08	0.16	0.06	0.10	0.12	0.13	0.07	0.13	0.09	0.08	0.04	0.06
HIP92895	-0.24	0.13	-0.09	0.14	0.05	0.00	0.27	-0.01	-0.16	-0.10	-0.02	0.04	-0.12	-0.05	-0.07	0.07	-0.13	-0.10	-0.07
	0.04	0.04	0.05	0.06	0.06	0.03	0.04	0.07	0.15	0.06	0.07	0.09	0.06	0.05	0.08	0.09	0.09	0.04	0.06
HIP94576	0.03	0.08	0.81	0.39	0.42	0.30	0.48	0.21	0.30	0.25	0.26	0.25	0.32	0.21	0.24	0.80	0.33	0.24	0.31
	0.05	0.04	0.30	0.05	0.10	0.05	0.12	0.07	0.18	0.07	0.06	0.13	0.06	0.06	0.09	0.10	0.06	0.04	0.15
HIP94951	-0.15	0.19	0.05	0.15	0.10	0.09	0.24	-0.01	-0.10	0.01	0.02	0.05	0.07	-0.02	-0.01	0.25	0.03	0.02	0.05
	0.04	0.04	0.06	0.07	0.02	0.03	0.08	0.07	0.12	0.06	0.06	0.09	0.06	0.05	0.06	0.09	0.04	0.04	0.12
HIP95124	0.09	0.06	0.32	-0.09	0.32	0.34	0.42	0.15	0.20	0.22	0.20	0.30	0.30	0.20	0.15	0.66	0.26	0.22	0.20
	0.07	0.04	0.04	0.39	0.03	0.04	0.08	0.07	0.17	0.07	0.07	0.11	0.07	0.06	0.06	0.11	0.06	0.04	0.17
HIP97938	0.02	0.15	0.01	0.29	0.14	0.05	-0.02	-0.05	-0.09	-0.10	0.06	0.16	0.09	-0.18	-0.25	0.00	0.01	-0.14	-0.05
	0.06	0.03	0.05	0.06	0.04	0.04	0.19	0.07	0.17	0.07	0.10	0.12	0.11	0.07	0.07	0.11	0.08	0.04	0.24
HIP99894	-0.22	0.04	-0.17	-0.12	-0.11	-0.17	-0.17	-0.13	-0.29	-0.21	-0.14	-0.13	-0.25	-0.16	-0.19	-0.11	-0.18	-0.26	-0.26
	0.05	0.04	0.07	0.06	0.05	0.03	0.06	0.07	0.08	0.08	0.07	0.07	0.06	0.05	0.07	0.11	0.04	0.04	0.07
HIP103527	-0.25	0.15	0.15	0.14	0.08	0.07	0.21	0.06	-0.06	0.01	0.11	0.11	0.08	0.06	0.15	0.21	0.06	0.00	-0.37
	0.05	0.04	0.06	0.19	0.05	0.04	0.06	0.07	0.12	0.06	0.07	0.09	0.06	0.05	0.14	0.10	0.08	0.04	0.18
HIP104202	-0.31	0.10	-0.13	0.04	-0.06	-0.11	0.22	-0.09	-0.19	-0.10	-0.03	0.01	-0.13	-0.13	-0.12	-0.01	-0.17	-0.17	0.14
	0.04	0.04	0.04	0.06	0.03	0.03	0.05	0.07	0.12	0.07	0.07	0.08	0.06	0.06	0.06	0.09	0.03	0.04	0.22
HIP107251	-0.07	1.12	0.16	0.36	0.27	0.25	0.64	0.06	0.34	0.36	0.28	0.31	0.34	0.20	0.15	0.44	0.28	0.24	0.04
	0.20	0.04	0.11	0.08	0.03	0.03	0.04	0.08	0.17	0.07	0.07	0.13	0.07	0.06	0.11	0.15	0.07	0.04	0.35
HIP109577	-0.04	-0.01	0.06	0.13	0.14	0.10	0.21	0.00	-0.04	0.01	0.04	0.12	0.06	0.02	0.02	0.33	0.05	0.03	-0.05
	0.04	0.04	0.06	0.11	0.02	0.03	0.11	0.06	0.13	0.06	0.06	0.09	0.06	0.05	0.06	0.10	0.05	0.04	0.06
HIP110813	-0.28	-0.06	-0.20	0.04	-0.07	-0.08	0.18	-0.12	-0.28	-0.14	-0.14	-0.06	-0.17	-0.21	-0.18	-0.06	-0.21	-0.20	-0.29
	0.09	0.04	0.08	0.05	0.05	0.03	0.09	0.07	0.11	0.06	0.07	0.07	0.07	0.05	0.06	0.09	0.06	0.04	0.06
HIP114855	0.10	-0.03	-0.18	0.28	0.17	0.16	0.58	-0.08	-0.08	-0.02	0.00	0.17	0.04	-0.08	0.00	0.39	0.08	-0.01	-0.04
	0.10	0.03	0.12	0.04	0.04	0.05	0.14	0.06	0.20	0.05	0.05	0.14	0.05	0.05	0.07	0.09	0.04	0.04	0.20
HIP116076	-0.07	0.15	-0.14	0.14	0.07	0.01	0.24	-0.16	-0.26	-0.18	0.03	0.09	-0.01	-0.29	-0.31	-0.14	-0.05	-0.20	-0.25
	0.08	0.03	0.05	0.06	0.04	0.03	0.15	0.07	0.16	0.05	0.10	0.11	0.12	0.07	0.05	0.09	0.07	0.03	0.10
HD17092	0.15	0.06	0.52	0.26	0.30	0.28	0.67	0.06	0.15	0.11	0.14	0.01	0.25	0.08	0.07	0.50	0.21	0.12	0.68
	0.13	0.03	0.28	0.06	0.03	0.05	0.05	0.08	0.26	0.06	0.09	0.10	0.10	0.07	0.07	0.13	0.08	0.04	0.24
BD+20 2457	-0.10	-0.29	-0.81	-0.46	-0.69	-0.57	0.12	-0.68	-0.77	-0.74	-0.50	-0.49	-0.58	-0.76	-0.20	-1.02	-0.65	-0.87	-0.91
	0.05	0.03	0.10	0.07	0.03	0.04	0.24	0.07	0.16	0.05	0.08	0.09	0.08	0.07	0.52	0.08	0.05	0.04	0.07
$\gamma$ 1 Leo	-0.07	-0.28	-0.27	0.00	-0.20	-0.28		-0.41	-0.41	-0.41	-0.36	-0.23	-0.41	-0.44	-0.47	-0.34	-0.35	-0.44	0.00
	0.05	0.03	0.07	0.05	0.05	0.03		0.08	0.23	0.05	0.09	0.11	0.09	0.07	0.07	0.09	0.06	0.04	0.42
HD240210	0.17	-0.11	0.27	-0.13	0.20	0.10	0.68	-0.25	-0.15	-0.23	0.07	0.00	0.03	-0.12	-0.14	0.42	0.10	-0.07	0.04
	0.05	0.03	0.26	0.05	0.13	0.08	0.05	0.18	0.37	0.07	0.09	0.19	0.11	0.07	0.13	0.11	0.13	0.04	0.11

Giant stars without planets

Table 2. continued.

Star	C I	O I	Na I	Mg I	Al I	Si I	S I	Ca I	Sc I	Sc II	Ti I	Ti II	V I	Cr I	Cr II	Mn I	Co I	Ni I	Zn I
HIP729	-0.03	-0.04	0.19	0.18	0.17	0.16	0.27	0.02	-0.05	0.00	0.02	0.12	0.02	0.02	0.03	0.43	0.08	0.02	-0.10
	0.04	0.04	0.07	0.10	0.05	0.04	0.12	0.07	0.17	0.06	0.07	0.13	0.07	0.06	0.07	0.10	0.05	0.04	0.15
HIP873	-0.08	-0.08	0.06	0.21	0.11	0.13	0.28	0.01	-0.05	0.00	0.02	0.16	0.02	0.02	0.04	0.40	0.03	0.03	-0.03
	0.04	0.04	0.05	0.10	0.03	0.04	0.14	0.06	0.16	0.06	0.07	0.11	0.07	0.05	0.08	0.11	0.05	0.04	0.08
HIP6682	-0.07	-0.02	0.02	0.20	0.14	0.12	0.25	-0.04	0.01	0.00	0.04	0.11	0.07	-0.02	-0.07	0.13	0.04	0.00	-0.06
	0.08	0.03	0.04	0.07	0.03	0.04	0.10	0.06	0.16	0.05	0.05	0.11	0.05	0.05	0.08	0.26	0.04	0.04	0.06
HIP6999	-0.09	0.04	0.39	0.19	0.20	0.19	0.33	0.05	-0.06	0.07	0.05	0.18	0.09	0.05	0.06	0.42	0.13	0.07	0.00
	0.04	0.04	0.16	0.15	0.05	0.04	0.06	0.07	0.14	0.06	0.06	0.12	0.06	0.05	0.08	0.09	0.04	0.04	0.11
HIP7097	-0.42	-0.20	0.14	-0.05	-0.07	0.03	0.10	-0.14	-0.33	-0.21	-0.11	-0.22	-0.11	-0.18	-0.10	0.09	-0.14	-0.17	0.20
	0.15	0.03	0.08	0.13	0.12	0.04	0.18	0.07	0.18	0.09	0.09	0.12	0.10	0.07	0.19	0.11	0.07	0.04	0.40
HIP7607	0.29	0.02	0.24	0.03	0.33	0.28	1.11	-0.13	-0.06	0.08	0.13	0.22	0.34	0.00	0.07	0.83	0.40	0.19	0.25
	0.05	0.03	0.04	0.05	0.04	0.05	0.07	0.18	0.34	0.06	0.09	0.19	0.12	0.07	0.10	0.11	0.17	0.04	0.40
HIP7719	-0.37	-0.20	0.12	-0.02	-0.07	-0.07	0.03	-0.04	-0.31	-0.24	-0.13	-0.12	-0.21	-0.11	-0.02	0.02	-0.23	-0.21	-0.37
	0.05	0.04	0.07	0.06	0.02	0.03	0.06	0.07	0.12	0.06	0.07	0.09	0.06	0.05	0.17	0.10	0.05	0.04	0.08
HIP9222	-0.17	-0.10	-0.09	0.04	0.01	0.00	0.20	-0.10	-0.16	-0.09	-0.08	0.05	-0.10	-0.14	-0.18	0.06	-0.11	-0.15	-0.29
	0.09	0.03	0.04	0.13	0.05	0.03	0.09	0.07	0.16	0.05	0.08	0.10	0.09	0.06	0.06	0.10	0.06	0.04	0.11
HIP13531	-0.45	-0.26	0.07	-0.17	-0.14	-0.11	-0.01	-0.14	-0.34	-0.28	-0.27	-0.26	-0.33	-0.28	-0.21	-0.22	-0.30	-0.28	-0.34
	0.05	0.04	0.07	0.10	0.02	0.03	0.06	0.07	0.11	0.07	0.07	0.10	0.06	0.06	0.18	0.09	0.04	0.04	0.06
HIP19038	-0.05	0.08	0.27	0.34	0.21	0.23	0.40	0.03	0.03	0.11	0.09	0.22	0.12	0.06	0.07	0.55	0.16	0.11	0.06
	0.08	0.04	0.07	0.05	0.05	0.05	0.11	0.08	0.20	0.06	0.08	0.13	0.08	0.06	0.07	0.09	0.08	0.04	0.23
HIP42528	-0.02	0.23	0.23	0.17	0.06	0.08	0.59	0.02	-0.08	0.03	0.05	0.07	0.05	0.05	-0.03	0.07	0.01	-0.01	-0.08
	0.13	0.04	0.05	0.14	0.02	0.03	0.04	0.06	0.08	0.06	0.06	0.09	0.06	0.05	0.08	0.12	0.03	0.04	0.09
HIP59285	0.01	0.10	0.42	0.16	0.32	0.21	0.67	-0.04	0.25	0.10	0.14	0.28	0.21	0.01	0.18	0.65	0.22	0.09	0.23
	0.05	0.03	0.25	0.05	0.04	0.05	0.14	0.08	0.25	0.05	0.09	0.15	0.09	0.07	0.08	0.13	0.07	0.04	0.28
HIP59646	0.00	0.26	0.15	0.21	0.12	0.17	0.25	0.06	-0.02	0.06	0.07	0.16	0.05	0.11	0.11	0.43	0.04	0.08	0.13
	0.04	0.03	0.05	0.06	0.05	0.03	0.08	0.06	0.11	0.05	0.06	0.08	0.06	0.05	0.19	0.07	0.06	0.04	0.06
HIP59847	-0.30	-0.13	-0.05	-0.13	-0.06	-0.09	0.22	-0.14	-0.42	-0.29	-0.25	-0.18	-0.31	-0.22	-0.03	-0.14	-0.29	-0.27	-0.34
	0.14	0.03	0.08	0.20	0.04	0.03	0.13	0.07	0.10	0.05	0.09	0.10	0.09	0.07	0.25	0.11	0.04	0.03	0.10
HIP59856	-0.08	0.09	-0.02	0.07	0.05	0.05	0.47	-0.20	-0.15	-0.10	-0.11	0.14	-0.12	-0.19	0.03	0.12	-0.09	-0.13	0.07
	0.05	0.03	0.08	0.06	0.06	0.05	0.11	0.08	0.16	0.05	0.10	0.14	0.11	0.08	0.06	0.11	0.07	0.04	0.05
HIP68904	0.14	-0.08	0.26	0.02	0.25	0.10	0.32	0.06	0.14	0.00	0.11	0.06	0.28	0.11	0.04	0.42	0.04	0.03	-0.01
	0.04	0.04	0.13	0.05	0.05	0.03	0.12	0.08	0.13	0.06	0.07	0.10	0.06	0.06	0.08	0.08	0.06	0.04	0.16
HIP69185	-0.28	-0.21	-0.26	-0.10	-0.18	-0.20	0.05	-0.20	-0.41	-0.32	-0.25	-0.21	-0.34	-0.29	-0.25	-0.22	-0.31	-0.32	-0.32
	0.05	0.04	0.06	0.06	0.03	0.03	0.15	0.07	0.09	0.06	0.06	0.07	0.06	0.05	0.06	0.10	0.04	0.04	0.08
HIP69427	0.12	-0.23	-0.37	-0.18	-0.08	-0.22		-0.46	-0.11	-0.34	-0.15	-0.15	0.02	-0.40	-0.43	-0.21	-0.24	-0.37	-0.53
	0.05	0.03	0.07	0.05	0.05	0.03		0.14	0.30	0.05	0.09	0.14	0.11	0.07	0.10	0.09	0.07	0.04	0.22
HIP69612	-0.15	-0.01	0.02	0.10	0.05	0.06	0.22	-0.09	-0.21	-0.09	-0.03	0.05	-0.03	-0.11	-0.14	0.22	-0.02	-0.07	-0.02
	0.06	0.03	0.05	0.08	0.05	0.05	0.15	0.07	0.13	0.06	0.09	0.12	0.10	0.06	0.07	0.09	0.06	0.04	0.12
HIP70027	0.38	0.22	0.40	0.16	0.48	0.43	1.02	0.08	0.45	0.24	0.31	0.41	0.62	0.17	0.19	0.98	0.54	0.29	0.39
	0.07	0.03	0.08	0.06	0.08	0.06	0.07	0.15	0.34	0.07	0.10	0.19	0.12	0.07	0.15	0.13	0.17	0.04	0.35
HIP70038	-0.30	0.05	0.13	0.07	0.00	0.02	0.10	-0.05	-0.20	-0.12	-0.06	-0.01	-0.08	-0.03	-0.03	0.14	-0.09	-0.09	-0.17
	0.06	0.04	0.07	0.09	0.05	0.04	0.05	0.06	0.10	0.06	0.06	0.09	0.06	0.05	0.14	0.10	0.05	0.04	0.07
HIP80816	-0.28	-0.09	0.12	0.06	-0.06	0.01	0.00	-0.05	-0.30	-0.21	-0.11	-0.05	-0.19	-0.13	-0.02	0.03	-0.16	-0.16	-0.09
	0.09	0.04	0.07	0.06	0.07	0.04	0.08	0.07	0.12	0.06	0.07	0.09	0.08	0.06	0.13	0.09	0.05	0.04	0.11

Table 2. continued.

Star	C I	O I	Na I	Mg I	Al I	Si I	S I	Ca I	Sc I	Sc II	Ti I	Ti II	V I	Cr I	Cr II	Mn I	Co I	Ni I	Zn I
HIP84975	-0.22	0.02	-0.12	0.04	-0.06	-0.08	0.12	-0.13	-0.27	-0.12	-0.12	-0.02	-0.13	-0.18	-0.14	-0.03	-0.13	-0.17	-0.30
	0.05	0.04	0.04	0.06	0.02	0.03	0.07	0.07	0.12	0.06	0.06	0.08	0.06	0.05	0.06	0.09	0.05	0.04	0.06
HIP88765	-0.24	-0.01	0.21	0.17	0.06	0.10	0.23	0.02	-0.15	-0.07	-0.03	0.05	-0.03	-0.02	0.10	0.25	-0.04	-0.04	-0.17
	0.04	0.04	0.05	0.06	0.02	0.04	0.08	0.07	0.12	0.06	0.06	0.10	0.06	0.05	0.17	0.09	0.05	0.04	0.08
HIP88836	0.21	0.09	0.41	0.25	0.47	0.39	0.79	0.12	0.43	0.22	0.24	0.19	0.46	0.16	0.19	0.87	0.30	0.26	0.34
	0.06	0.03	0.05	0.06	0.05	0.06	0.12	0.08	0.31	0.07	0.09	0.12	0.10	0.07	0.09	0.11	0.07	0.04	0.31
HIP89826	0.06	0.11	0.58	0.23	0.24	0.35	0.56	0.03	0.11	0.10	0.11	0.16	0.28	0.07	0.14	0.65	0.29	0.15	0.10
	0.06	0.03	0.28	0.06	0.04	0.06	0.18	0.09	0.25	0.06	0.09	0.14	0.10	0.07	0.07	0.09	0.10	0.04	0.30
HIP89918	-0.28	-0.02	0.12	0.07	-0.03	-0.03	0.08	-0.02	-0.28	-0.16	-0.11	-0.05	-0.15	-0.11	0.05	0.07	-0.15	-0.14	-0.17
	0.05	0.04	0.07	0.09	0.05	0.03	0.06	0.07	0.10	0.06	0.06	0.09	0.06	0.05	0.12	0.09	0.05	0.04	0.07
HIP89962	-0.24	-0.05	-0.14	-0.05	-0.05	-0.10	0.09	-0.14	-0.25	-0.18	-0.13	-0.05	-0.15	-0.20	-0.22	-0.02	-0.16	-0.20	-0.28
	0.07	0.04	0.04	0.12	0.04	0.03	0.11	0.07	0.08	0.06	0.06	0.09	0.06	0.05	0.06	0.09	0.05	0.04	0.07
HIP95822	-0.09	0.11	0.16	0.29	0.16	0.18	0.27	0.06	-0.01	0.05	0.09	0.19	0.09	0.06	0.03	0.48	0.11	0.06	0.53
	0.07	0.04	0.05	0.05	0.03	0.04	0.08	0.07	0.16	0.06	0.08	0.13	0.08	0.06	0.08	0.09	0.06	0.04	0.52
HIP95926	-0.03	-0.09	-0.06	0.21	0.05	0.03	0.25	-0.10	-0.14	-0.06	-0.05	0.01	-0.05	-0.08	0.01	0.19	-0.06	-0.05	-0.08
	0.08	0.04	0.04	0.05	0.03	0.03	0.04	0.07	0.12	0.05	0.07	0.09	0.07	0.06	0.10	0.10	0.05	0.04	0.06
HIP96016	-0.23	-0.11	-0.11	0.07	-0.06	-0.05	0.04	-0.08	-0.24	-0.14	-0.09	-0.03	-0.15	-0.14	-0.13	0.05	-0.15	-0.15	0.15
	0.05	0.04	0.05	0.08	0.02	0.03	0.07	0.07	0.14	0.06	0.06	0.08	0.06	0.05	0.06	0.10	0.04	0.04	0.33
HIP96229	0.44	0.10	0.54	0.24	0.47	0.33	0.90	-0.02	0.49	0.25	0.32	0.30	0.44	0.10	0.14	0.80	0.35	0.20	0.41
	0.07	0.03	0.32	0.05	0.03	0.05	0.10	0.15	0.35	0.05	0.10	0.16	0.10	0.07	0.09	0.10	0.08	0.04	0.33
HIP98210	-0.16	-0.03	-0.12	0.11	0.01	-0.06	0.24	-0.13	-0.18	-0.13	-0.10	-0.01	-0.09	-0.18	-0.15	-0.01	-0.11	-0.16	-0.05
	0.06	0.04	0.05	0.05	0.03	0.03	0.12	0.07	0.14	0.05	0.07	0.09	0.08	0.06	0.06	0.09	0.05	0.04	0.15
HIP98314	-0.42	-0.19	-0.26	-0.15	-0.22	-0.24	-0.15	-0.26	-0.40	-0.32	-0.27	-0.22	-0.34	-0.37	-0.36	-0.34	-0.31	-0.37	-0.37
	0.04	0.04	0.06	0.05	0.02	0.03	0.04	0.07	0.10	0.06	0.06	0.08	0.05	0.05	0.08	0.09	0.05	0.04	0.06
HIP98845	-0.16	-0.17	-0.11	0.02	-0.16	-0.23	-0.08	-0.18	-0.26	-0.26	-0.11	-0.22	-0.23	-0.25	-0.31	-0.16	-0.26	-0.33	-0.18
	0.05	0.04	0.06	0.07	0.07	0.03	0.04	0.07	0.07	0.06	0.07	0.08	0.06	0.05	0.12	0.09	0.06	0.04	0.06
HIP98920	0.12	0.08	0.26	0.41	0.25	0.18	0.34	0.08	0.12	0.09	0.14	0.24	0.16	0.10	0.07	0.53	0.16	0.11	0.21
	0.24	0.04	0.06	0.05	0.08	0.05	0.09	0.07	0.25	0.06	0.08	0.13	0.08	0.06	0.10	0.12	0.05	0.04	0.13
HIP99171	0.16	0.09	0.10	0.24	0.25	0.12	0.41	-0.06	0.16	0.07	0.14	0.16	0.12	-0.05	-0.01	0.29	0.05	0.01	0.12
	0.05	0.04	0.07	0.05	0.03	0.03	0.06	0.07	0.22	0.06	0.07	0.10	0.09	0.06	0.06	0.11	0.05	0.04	0.10
HIP99841	-0.33	-0.07	0.05	0.06	-0.02	-0.02	0.04	-0.08	-0.25	-0.12	-0.09	-0.01	-0.14	-0.12	-0.13	0.07	-0.13	-0.15	-0.22
	0.06	0.04	0.04	0.07	0.03	0.04	0.10	0.06	0.12	0.06	0.06	0.09	0.05	0.05	0.06	0.10	0.05	0.04	0.06
HIP99913	-0.04	-0.01	0.17	0.24	0.15	0.18	0.38	0.05	0.00	0.05	0.07	0.24	0.08	0.06	-0.05	0.47	0.07	0.08	0.08
	0.05	0.04	0.07	0.09	0.03	0.04	0.08	0.07	0.18	0.06	0.08	0.13	0.09	0.06	0.18	0.12	0.06	0.04	0.11
HIP100022	0.13	-0.08	0.41	0.31	0.32	0.27	0.45	0.08	0.27	0.19	0.20	0.20	0.30	0.16	0.14	0.68	0.25	0.22	0.16
	0.06	0.04	0.18	0.05	0.02	0.04	0.07	0.07	0.20	0.07	0.07	0.11	0.07	0.06	0.07	0.11	0.05	0.04	0.10
HIP100503	-0.28	-0.16	-0.20	-0.08	-0.16	-0.15	0.09	-0.18	-0.34	-0.25	-0.18	-0.12	-0.25	-0.22	-0.15	-0.14	-0.25	-0.27	-0.37
	0.05	0.03	0.05	0.05	0.04	0.03	0.08	0.07	0.07	0.06	0.06	0.07	0.06	0.05	0.07	0.08	0.05	0.04	0.06
HIP100541	-0.16	0.02	0.09	0.10	0.01	0.06	0.24	-0.08	-0.23	-0.07	-0.09	0.05	-0.10	-0.09	-0.08	0.16	-0.07	-0.07	-0.11
	0.05	0.04	0.06	0.09	0.02	0.04	0.05	0.06	0.11	0.06	0.06	0.11	0.06	0.05	0.06	0.10	0.05	0.04	0.09
HIP100587	0.33	-0.06	0.28	-0.15	0.15	0.17	0.76	-0.29	-0.08	-0.04	0.05	0.15	0.09	-0.04	-0.04	0.62	0.11	0.06	0.21
	0.04	0.03	0.26	0.05	0.03	0.05	0.04	0.20	0.42	0.06	0.07	0.19	0.06	0.06	0.10	0.14	0.06	0.05	0.05
HIP101848	-0.18	-0.31	-0.12	0.02	-0.06	-0.07	0.11	-0.12	-0.23	-0.22	-0.12	-0.09	-0.16	-0.16	-0.16	0.02	-0.17	-0.21	-0.20
	0.04	0.04	0.04	0.06	0.02	0.03	0.05	0.07	0.07	0.05	0.06	0.07	0.06	0.05	0.06	0.09	0.06	0.04	0.08

Table 2. continued.

Star	C I	O I	Na I	Mg I	Al I	Si I	S I	Ca I	Sc I	Sc II	Ti I	Ti II	V I	Cr I	Cr II	Mn I	Co I	Ni I	Zn I
HIP101936	-0.04	-0.01	0.19	0.22	0.14	0.22	0.37	0.03	-0.04	0.04	0.02	0.19	0.03	0.03	0.04	0.50	0.12	0.06	-0.03
	0.06	0.04	0.07	0.11	0.06	0.05	0.08	0.07	0.18	0.06	0.08	0.14	0.08	0.06	0.06	0.10	0.05	0.04	0.11
HIP102532	0.00	0.08	0.29	0.33	0.28	0.25	0.48	0.09	0.17	0.13	0.13	0.26	0.16	0.09	0.10	0.60	0.19	0.16	-0.03
	0.08	0.04	0.10	0.05	0.04	0.04	0.14	0.07	0.22	0.06	0.07	0.13	0.07	0.06	0.10	0.10	0.06	0.04	0.21
HIP103004	-0.26	-0.03	0.16	-0.01	0.15	0.01	0.02	-0.01	-0.13	-0.12	-0.07	-0.02	-0.09	-0.07	0.05	0.07	-0.13	-0.12	0.04
	0.04	0.03	0.06	0.05	0.18	0.03	0.04	0.06	0.08	0.06	0.06	0.09	0.06	0.05	0.15	0.09	0.06	0.04	0.30
HIP103519	-0.06	0.06	0.34	0.26	0.20	0.23	0.32	0.08	0.03	0.10	0.09	0.17	0.13	0.11	0.11	0.56	0.16	0.13	0.00
	0.06	0.04	0.10	0.06	0.03	0.04	0.05	0.06	0.14	0.07	0.06	0.11	0.07	0.05	0.08	0.09	0.05	0.04	0.15
HIP105390	-0.13	-0.42	-0.16	-0.02	-0.14	-0.12	-0.09	-0.16	-0.33	-0.23	-0.18	-0.14	-0.22	-0.22	-0.18	-0.14	-0.21	-0.26	-0.28
	0.08	0.04	0.04	0.06	0.02	0.03	0.04	0.07	0.09	0.06	0.06	0.07	0.06	0.05	0.06	0.08	0.03	0.04	0.07
HIP105411	0.05	0.48	0.03	0.24	0.20	0.09	0.31	-0.03	0.01	0.00	0.14	0.20	0.12	-0.15	-0.19	0.20	0.11	-0.08	0.04
	0.08	0.03	0.08	0.06	0.04	0.04	0.05	0.07	0.17	0.05	0.09	0.12	0.09	0.06	0.07	0.09	0.06	0.04	0.06
HIP105502	0.08	0.07	0.16	0.13	0.16	0.17	0.33	-0.02	-0.04	-0.01	0.03	0.07	0.02	-0.05	-0.01	0.40	0.06	-0.01	0.51
	0.03	0.03	0.19	0.11	0.02	0.05	0.13	0.06	0.19	0.06	0.06	0.11	0.05	0.05	0.08	0.09	0.05	0.04	0.35
HIP106081	0.15	0.04	0.21	0.27	0.30	0.24	0.50	0.01	0.18	0.14	0.14	0.25	0.16	0.07	0.12	0.60	0.19	0.16	0.02
	0.07	0.03	0.07	0.05	0.04	0.05	0.06	0.08	0.25	0.06	0.08	0.14	0.08	0.06	0.07	0.12	0.05	0.04	0.30
HIP106093	-0.09	0.01	0.21	0.21	0.12	0.17	0.28	0.04	-0.09	0.01	0.01	0.15	0.04	0.03	0.00	0.41	0.04	0.03	0.43
	0.07	0.04	0.06	0.09	0.03	0.04	0.11	0.06	0.13	0.07	0.06	0.11	0.06	0.05	0.06	0.10	0.05	0.04	0.34
HIP110538	-0.31	-0.15	-0.20	-0.09	-0.14	-0.16	0.16	-0.24	-0.39	-0.26	-0.26	-0.11	-0.32	-0.32	-0.24	-0.17	-0.27	-0.29	-0.33
	0.06	0.03	0.06	0.09	0.04	0.03	0.06	0.07	0.15	0.05	0.10	0.09	0.11	0.07	0.06	0.09	0.06	0.03	0.05
HIP111944	0.03	-0.12	0.12	-0.04	-0.03	-0.07	0.47	-0.32	-0.14	-0.27	-0.15	-0.06	0.07	-0.23	-0.26	0.16	-0.09	-0.22	-0.44
	0.05	0.03	0.19	0.05	0.03	0.05	0.06	0.14	0.27	0.05	0.08	0.15	0.10	0.07	0.11	0.09	0.08	0.04	0.30
HIP112041	-0.33	-0.29	-0.27	-0.18	-0.22	-0.28	-0.11	-0.33	-0.45	-0.38	-0.35	-0.26	-0.40	-0.44	-0.41	-0.38	-0.36	-0.42	-0.42
	0.06	0.03	0.08	0.07	0.04	0.03	0.06	0.07	0.12	0.04	0.09	0.07	0.11	0.07	0.05	0.09	0.06	0.03	0.05
HIP112067	0.04	-0.14	0.10	0.09	0.13	0.15	0.51	-0.09	-0.03	0.01	0.04	0.01	0.07	-0.09	0.14	0.54	0.10	-0.03	0.05
	0.06	0.04	0.13	0.05	0.05	0.06	0.32	0.06	0.20	0.09	0.07	0.14	0.07	0.06	0.31	0.09	0.06	0.04	0.08
HIP112158	-0.42	-0.25	0.03	-0.13	-0.12	-0.11	-0.03	-0.12	-0.41	-0.27	-0.24	-0.19	-0.31	-0.24	-0.19	-0.26	-0.30	-0.28	-0.20
	0.05	0.03	0.05	0.07	0.04	0.03	0.05	0.08	0.13	0.06	0.08	0.10	0.08	0.06	0.14	0.08	0.05	0.04	0.22
HIP112242	-0.16	0.11	0.51	0.23	0.18	0.25	0.34	0.08	-0.02	0.10	0.05	0.18	0.10	0.09	0.24	0.44	0.12	0.11	0.03
	0.04	0.04	0.10	0.09	0.05	0.04	0.08	0.07	0.14	0.07	0.06	0.11	0.07	0.05	0.21	0.09	0.05	0.04	0.07
HIP115696	-0.25	-0.16	-0.29	-0.17	-0.21	-0.26	-0.03	-0.34	-0.42	-0.35	-0.31	-0.21	-0.37	-0.41	-0.34	-0.39	-0.34	-0.38	-0.32
	0.04	0.04	0.05	0.10	0.03	0.03	0.04	0.07	0.11	0.06	0.07	0.08	0.06	0.05	0.06	0.09	0.06	0.04	0.07
HIP115830	0.01	0.08	0.41	0.28	0.18	0.21	0.37	0.01	0.00	0.07	0.08	0.20	0.05	0.04	0.05	0.52	0.15	0.10	0.11
	0.08	0.03	0.24	0.06	0.03	0.05	0.14	0.07	0.20	0.06	0.09	0.14	0.09	0.07	0.09	0.11	0.08	0.03	0.07
HIP115919	-0.21	-0.03	0.21	0.20	0.11	0.12	0.21	0.04	-0.12	-0.01	0.03	0.10	0.02	0.03	0.21	0.35	0.02	0.02	-0.02
	0.06	0.04	0.07	0.08	0.02	0.04	0.06	0.06	0.13	0.06	0.06	0.11	0.06	0.05	0.25	0.09	0.03	0.04	0.07
HIP116584	-0.18	-0.02	-0.23	-0.12	0.09	-0.22	0.05	-0.21	-0.17	-0.22	-0.03	-0.05	-0.07	-0.38	-0.55	-0.40	-0.21	-0.41	-0.07
	0.04	0.04	0.06	0.08	0.11	0.03	0.04	0.07	0.16	0.07	0.07	0.10	0.07	0.06	0.09	0.08	0.06	0.04	0.35
HIP116823	0.32	0.14	0.05	0.16	0.46	0.30	0.97	-0.03	0.47	0.22	0.30	0.28	0.43	0.11	0.12	0.79	0.30	0.20	0.25
	0.05	0.03	0.21	0.06	0.03	0.05	0.07	0.14	0.35	0.07	0.09	0.16	0.10	0.07	0.07	0.11	0.06	0.04	0.24
HIP117375	-0.29	-0.10	-0.03	0.12	0.06	0.07	0.15	0.01	-0.24	-0.10	-0.05	-0.01	-0.11	-0.09	0.06	0.17	-0.08	-0.09	-0.09
	0.07	0.04	0.09	0.11	0.04	0.04	0.08	0.07	0.10	0.07	0.07	0.10	0.06	0.05	0.14	0.09	0.04	0.04	0.17
HIP117411	0.23	0.09	0.52	0.30	0.34	0.31	0.65	0.05	0.35	0.21	0.18	0.30	0.26	0.13	0.18	0.75	0.27	0.25	0.26
	0.06	0.03	0.23	0.05	0.04	0.04	0.14	0.08	0.26	0.06	0.08	0.13	0.07	0.07	0.08	0.12	0.05	0.04	0.22



Table 2. continued.

Star	C I	O I	Na I	Mg I	Al I	Si I	S I	Ca I	Sc I	Sc II	Ti I	Ti II	V I	Cr I	Cr II	Mn I	Co I	Ni I	Zn I
HIP117541	0.11	0.07	0.27	0.29	0.28	0.26	0.56	0.00	0.12	0.09	0.18	0.21	0.23	0.00	0.05	0.58	0.22	0.11	0.14
	0.10	0.03	0.24	0.06	0.05	0.05	0.09	0.08	0.25	0.06	0.10	0.13	0.10	0.07	0.08	0.09	0.07	0.04	0.20
Subgiant stars with planets																			
HIP8159	0.04	0.02	0.14	0.23	0.18	0.13	0.00	0.11	0.03	0.09	0.08	0.08	0.07	0.09	0.09	0.27	0.08	0.09	0.01
	0.02	0.01	0.02	0.04	0.02	0.02	0.11	0.04	0.02	0.04	0.03	0.04	0.03	0.03	0.04	0.07	0.06	0.02	0.05
HIP12048	0.06	-0.05	0.08	0.21	0.13	0.09	0.07	0.10	0.11	0.03	0.10	0.10	0.05	0.12	0.20	0.19	0.05	0.08	0.10
	0.01	0.01	0.02	0.02	0.02	0.01	0.10	0.04	0.02	0.03	0.02	0.04	0.02	0.02	0.08	0.05	0.05	0.02	0.19
HIP12191	0.24	-0.31	0.40	0.28	0.31	0.29	0.12	0.26	0.24	0.29	0.22	0.26	0.27	0.23	0.36	0.51	0.21	0.30	0.20
	0.03	0.01	0.01	0.06	0.01	0.01	0.22	0.04	0.06	0.04	0.02	0.04	0.03	0.02	0.10	0.08	0.04	0.02	0.08
HIP27253	0.25	0.14	0.44	0.40	0.36	0.36	0.35	0.25	0.26	0.34	0.29	0.32	0.31	0.29	0.32	0.57	0.33	0.34	0.20
	0.02	0.02	0.03	0.06	0.01	0.02	0.06	0.04	0.04	0.04	0.03	0.06	0.03	0.03	0.04	0.07	0.04	0.02	0.07
HIP36795	-0.21		-0.11	-0.23	-0.22	-0.15	-0.03	-0.13	-0.01	-0.31	-0.22	-0.26	-0.03	-0.26	-0.22	-0.33	-0.31	-0.28	-0.34
	0.02		0.10	0.06	0.01	0.02	0.01	0.04	0.01	0.05	0.03	0.04	0.18	0.03	0.06	0.05	0.05	0.03	0.05
HIP42446	0.50		0.37	0.43	0.37	0.33	0.28	0.21	0.45	0.23	0.39	0.43	0.48	0.27	0.49	0.64	0.34	0.34	0.15
	0.19		0.04	0.05	0.04	0.03	0.19	0.06	0.16	0.09	0.07	0.13	0.07	0.06	0.46	0.13	0.04	0.05	0.05
HIP49813	0.21	0.09	0.38	0.45	0.38	0.36	0.35	0.24	0.22	0.26	0.28	0.31	0.30	0.29	0.26	0.63	0.31	0.32	0.46
	0.04	0.02	0.02	0.07	0.02	0.03	0.06	0.05	0.06	0.05	0.04	0.06	0.04	0.04	0.08	0.09	0.04	0.03	0.28
HIP54195	0.26		0.43	0.40	0.39	0.36	0.36	0.26	0.26	0.36	0.27	0.30	0.32	0.29	0.37	0.49	0.29	0.35	0.28
	0.04		0.04	0.06	0.01	0.01	0.09	0.04	0.03	0.04	0.02	0.06	0.02	0.03	0.09	0.05	0.04	0.02	0.08
HIP66192	0.28	0.15	0.22	0.26	0.23	0.20	0.23	0.17	0.13	0.20	0.17	0.12	0.19	0.17	0.24	0.41	0.18	0.22	0.14
	0.08	0.01	0.09	0.02	0.01	0.02	0.07	0.04	0.02	0.05	0.02	0.05	0.03	0.02	0.09	0.08	0.04	0.02	0.12
HIP93746	0.46	0.77	0.56	0.48	0.63	0.51	0.75	0.16	0.77	0.62	0.49	0.54	0.60	0.41	0.49	0.96	0.56	0.52	0.56
	0.14	0.03	0.08	0.05	0.06	0.04	0.35	0.08	0.26	0.09	0.08	0.14	0.06	0.06	0.07	0.11	0.07	0.05	0.40
HIP94256	0.26		0.26	0.39	0.41	0.33	0.16	0.26	0.42	0.41	0.36	0.34	0.41	0.31	0.33	0.39	0.41	0.35	0.09
	0.08		0.12	0.14	0.03	0.02	0.03	0.04	0.04	0.05	0.02	0.05	0.03	0.03	0.04	0.10	0.07	0.03	0.21
HIP96507	0.14	0.26	0.24	0.18	0.26	0.20	0.06	0.17	0.35	0.20	0.18	0.14	0.20	0.13	0.27	0.20	0.00	0.13	0.18
	0.10	0.02	0.07	0.04	0.11	0.01	0.09	0.04	0.07	0.05	0.03	0.04	0.04	0.03	0.07	0.07	0.17	0.03	0.11
HIP100970	-0.02	0.30	0.04	0.14	0.14	0.04	0.10	0.12	0.02	0.02	0.02	0.01	0.03	0.08	0.33	0.14	-0.04	0.01	-0.08
	0.03	0.01	0.01	0.04	0.09	0.02	0.12	0.04	0.03	0.05	0.03	0.04	0.04	0.03	0.18	0.05	0.03	0.02	0.07
HIP114699	-0.14	-0.06	-0.21	-0.01	-0.03	-0.11	0.02	-0.12	-0.21	-0.15	-0.11	-0.09	-0.18	-0.18	-0.14	-0.20	-0.19	-0.22	-0.05
	0.03	0.03	0.03	0.04	0.04	0.02	0.03	0.05	0.06	0.04	0.05	0.05	0.05	0.04	0.05	0.06	0.04	0.03	0.24
HIP115100	0.09	0.96	0.20	0.22	0.19	0.15	0.09	0.11	0.10	0.15	0.10	0.13	0.12	0.08	0.16	0.21	0.10	0.12	0.11
	0.01	0.01	0.01	0.02	0.01	0.01	0.09	0.04	0.01	0.04	0.02	0.04	0.02	0.02	0.06	0.06	0.04	0.02	0.07
HIP118319	0.22	0.23	0.33	0.23	0.21	0.27	0.22	0.16	0.25	0.27	0.21	0.20	0.21	0.19	0.31	0.33	0.21	0.25	0.23
	0.01	0.02	0.01	0.02	0.01	0.01	0.15	0.04	0.01	0.04	0.02	0.04	0.03	0.02	0.10	0.04	0.04	0.02	0.21
HAT-P-7	-0.06	-0.28	0.06	0.15	0.03	0.19	-0.11	0.26		0.18	0.27	0.22	0.35	0.25	0.15	0.04	0.16	0.22	-0.17
	0.04	0.02	0.02	0.04	0.05	0.03	0.18	0.04		0.04	0.03	0.04	0.07	0.04	0.06	0.08	0.10	0.03	0.15
Subgiant stars without planets																			
HIP6512	0.01	0.05	0.00	0.18	0.14	0.04	0.12	-0.04	-0.06	0.00	0.05	0.05	0.01	-0.07	-0.10	0.02	-0.02	-0.09	-0.04
	0.04	0.03	0.04	0.06	0.03	0.02	0.05	0.06	0.08	0.05	0.06	0.07	0.06	0.05	0.05	0.09	0.06	0.03	0.07
HIP12350	-0.02	-0.07	0.10	0.17	0.41	0.12	-0.02	0.12	0.04	0.14	0.11	0.16	0.11	0.09	0.04	0.11	0.05	0.09	-0.02
	0.05	0.01	0.02	0.03	0.21	0.02	0.02	0.04	0.04	0.04	0.03	0.04	0.03	0.03	0.08	0.04	0.03	0.02	0.07
HIP14086	-0.51	-0.23	-0.58	-0.29	-0.34	-0.41		-0.40	-0.51	-0.56	-0.37	-0.39	-0.52	-0.62	-0.56	-0.89	-0.57	-0.65	-0.51
	0.04	0.03	0.04	0.08	0.04	0.03		0.06	0.05	0.06	0.06	0.07	0.07	0.05	0.05	0.07	0.05	0.04	0.07

Table 2. continued.

Star	C I	O I	Na I	Mg I	Al I	Si I	S I	Ca I	Sc I	Sc II	Ti I	Ti II	V I	Cr I	Cr II	Mn I	Co I	Ni I	Zn I
HIP15776	-0.45	-0.34	-0.45	-0.37	-0.39	-0.45	-0.46	-0.40	-0.60	-0.55	-0.49	-0.48	-0.60	-0.56	-0.48	-0.69	-0.54	-0.58	-0.53
	0.03	0.02	0.06	0.06	0.02	0.02	0.03	0.06	0.03	0.05	0.05	0.05	0.04	0.04	0.05	0.06	0.04	0.03	0.06
HIP17183	0.04	-0.01	-0.01	0.11	0.75	0.07	0.08	0.03	0.18	0.07	0.18	0.11	0.13	0.02	0.07	0.17	0.05	-0.01	-0.15
	0.14	0.04	0.04	0.13	0.47	0.03	0.04	0.07	0.18	0.05	0.07	0.07	0.06	0.05	0.06	0.08	0.05	0.04	0.14
HIP17378	0.14	0.04	0.18	0.23	0.20	0.17	0.32	0.04	0.12	0.06	0.13	0.14	0.15	0.08	0.11	0.37	0.12	0.10	0.39
	0.04	0.03	0.04	0.05	0.03	0.03	0.11	0.06	0.12	0.05	0.06	0.09	0.06	0.05	0.07	0.08	0.05	0.04	0.28
HIP18432	-0.23	-0.12	-0.34	-0.13	-0.13	-0.24	-0.19	-0.26	-0.31	-0.32	-0.22	-0.22	-0.32	-0.36	-0.30	-0.47	-0.34	-0.38	-0.30
	0.04	0.03	0.03	0.06	0.02	0.02	0.03	0.05	0.04	0.05	0.05	0.05	0.05	0.04	0.05	0.06	0.05	0.03	0.07
HIP60585	0.31		0.29	0.32	0.32	0.24	0.00	0.29	0.42	0.27	0.32	0.36	0.24	0.32	0.48	0.35	0.22	0.22	0.18
	0.10		0.08	0.05	0.10	0.03	0.15	0.05	0.01	0.07	0.03	0.05	0.04	0.04	0.10	0.11	0.06	0.03	0.19
HIP64408	0.11	0.04	0.20	0.23	0.59	0.14	0.13	0.08	0.06	0.12	0.07	0.10	0.10	0.12	0.11	0.24	0.12	0.15	0.10
	0.02	0.01	0.05	0.02	0.03	0.01	0.04	0.04	0.02	0.04	0.02	0.04	0.02	0.02	0.04	0.04	0.05	0.02	0.09
HIP70616	0.37	0.09	0.76	0.38	0.58	0.46	0.73	0.24	0.63	0.47	0.43	0.33	0.58	0.36	0.42	0.95	0.54	0.45	0.53
	0.04	0.03	0.19	0.05	0.05	0.05	0.17	0.07	0.23	0.07	0.07	0.10	0.06	0.06	0.07	0.11	0.06	0.05	0.15
HIP81819	-0.01	0.10	-0.06	0.09	0.07	0.01	0.13	-0.02	-0.08	-0.02	-0.01	0.04	-0.02	-0.02	0.03	0.01	-0.04	-0.05	0.10
	0.04	0.02	0.02	0.03	0.02	0.02	0.08	0.04	0.04	0.04	0.03	0.05	0.03	0.03	0.08	0.05	0.04	0.03	0.25
HIP98036	-0.21	0.02	-0.18	-0.07	-0.11	-0.12	0.02	-0.17	-0.26	-0.18	-0.15	-0.10	-0.19	-0.19	-0.16	-0.12	-0.19	-0.22	-0.15
	0.06	0.03	0.04	0.05	0.04	0.03	0.04	0.06	0.07	0.06	0.06	0.07	0.06	0.05	0.07	0.08	0.05	0.04	0.06
HIP98138	0.03	0.04	0.23	0.04	0.07	0.08	0.05	0.09	0.05	0.03	0.04	0.03	-0.01	0.01	0.12	0.02	-0.03	0.00	-0.18
	0.16	0.01	0.13	0.05	0.01	0.02	0.14	0.04	0.03	0.04	0.03	0.04	0.03	0.04	0.05	0.04	0.06	0.02	0.11
HIP102531	-0.01	-0.16	0.13	0.05	0.08	0.12	-0.07	0.12	0.28	-0.02	0.05	0.01	0.06	0.06	0.16	0.07	0.02	0.07	0.01
	0.02	0.02	0.02	0.05	0.05	0.01	0.13	0.04	0.01	0.04	0.03	0.04	0.05	0.02	0.08	0.06	0.08	0.02	0.14
HIP109822	-0.10	0.01	-0.21	0.02	0.04	-0.09	0.14	-0.16	-0.14	-0.16	-0.05	-0.04	-0.12	-0.25	-0.22	-0.28	-0.17	-0.27	0.07
	0.16	0.04	0.05	0.05	0.04	0.03	0.04	0.06	0.12	0.05	0.07	0.07	0.06	0.05	0.06	0.08	0.05	0.04	0.25
HIP116250	0.27	0.19	0.39	0.36	0.39	0.32	0.18	0.26	0.27	0.36	0.25	0.31	0.30	0.25	0.23	0.37	0.32	0.34	0.21
	0.02	0.01	0.01	0.03	0.02	0.01	0.05	0.04	0.02	0.04	0.02	0.04	0.01	0.02	0.04	0.04	0.03	0.02	0.09
Main-sequence stars with planets																			
HIP20723	0.21		0.34	0.28	0.25	0.23	0.14	0.13	0.18	0.24	0.18	0.20	0.21	0.20	0.24	0.46	0.25	0.24	0.20
	0.04		0.02	0.05	0.02	0.01	0.09	0.04	0.03	0.04	0.03	0.04	0.03	0.02	0.04	0.08	0.05	0.02	0.08
HIP31246	0.28	0.35	0.37	0.32	0.37	0.31	0.27	0.13	0.34	0.34	0.29	0.34	0.39	0.27	0.34	0.57	0.36	0.34	0.63
	0.04	0.02	0.03	0.03	0.03	0.03	0.07	0.05	0.08	0.05	0.04	0.06	0.04	0.04	0.07	0.08	0.04	0.03	0.22
HIP60081	0.19	0.25	0.38	0.36	0.34	0.30	0.20	0.21	0.25	0.29	0.24	0.26	0.28	0.27	0.27	0.43	0.27	0.30	0.24
	0.02	0.01	0.01	0.04	0.02	0.01	0.06	0.04	0.01	0.04	0.02	0.04	0.02	0.02	0.04	0.04	0.04	0.02	0.08
HIP80838	0.48	1.29	0.54	0.27	0.45	0.40	0.00	0.38	0.78	0.77	0.52	0.53	0.58	0.48	0.83	0.71	0.58	0.49	0.59
	0.02	0.02	0.02	0.03	0.14	0.02	0.23	0.05	0.22	0.06	0.04	0.05	0.06	0.05	0.14	0.07	0.01	0.03	0.22
HIP95740	0.33		0.36	0.48	0.39	0.41	0.29	0.35	0.51	0.51	0.45	0.49	0.43	0.43	0.74	0.63	0.50	0.48	0.31
	0.02		0.11	0.04	0.13	0.02	0.21	0.06	0.14	0.07	0.03	0.05	0.04	0.02	0.18	0.11	0.07	0.02	0.09
HIP98767	0.23	0.14	0.26	0.37	0.34	0.27	0.23	0.17	0.25	0.29	0.29	0.30	0.30	0.23	0.22	0.38	0.29	0.23	0.20
	0.02	0.01	0.02	0.04	0.01	0.02	0.03	0.04	0.02	0.03	0.03	0.10	0.03	0.03	0.05	0.05	0.03	0.02	0.05
HIP109378	0.24	1.16	0.26	0.35	0.36	0.26	0.22	0.16	0.24	0.29	0.29	0.26	0.29	0.21	0.23	0.44	0.27	0.22	0.34
	0.03	0.02	0.02	0.02	0.02	0.02	0.06	0.04	0.06	0.03	0.03	0.04	0.03	0.03	0.04	0.08	0.05	0.02	0.17
HIP113357	0.18		0.15	0.25	0.21	0.20	0.13	0.13	0.13	0.18	0.16	0.15	0.18	0.18	0.18	0.34	0.24	0.20	0.16
	0.02		0.10	0.02	0.02	0.01	0.09	0.04	0.01	0.05	0.02	0.03	0.02	0.02	0.03	0.04	0.02	0.02	0.04
HIP113421	0.28	0.27	0.44	0.44	0.40	0.35	0.27	0.23	0.32	0.36	0.35	0.34	0.39	0.35	0.38	0.56	0.37	0.37	0.27

**Table 2.** continued.

Star	C I	O I	Na I	Mg I	Al I	Si I	S I	Ca I	Sc I	Sc II	Ti I	Ti II	V I	Cr I	Cr II	Mn I	Co I	Ni I	Zn I
	0.02	0.01	0.03	0.05	0.02	0.01	0.05	0.04	0.06	0.04	0.03	0.04	0.03	0.02	0.06	0.06	0.05	0.02	0.11
GSC02883 <sup>†</sup>	0.18	0.66	0.36	0.34	0.36	0.31	0.08	0.22	0.38	0.33	0.33	0.23	0.28	0.30	0.36	0.42	0.30	0.32	0.43
	0.03	0.01	0.02	0.11	0.02	0.03	0.25	0.04	0.06	0.06	0.03	0.08	0.03	0.02	0.32	0.13	0.03	0.03	0.11
TrES-4	0.34	0.77	0.40	0.23	0.01	0.36	-0.19	0.29	0.57	0.29	0.50	0.39	0.54	0.46	0.37	0.38	0.13	0.39	0.25
	0.12	0.02	0.03	0.05	0.43	0.02	0.39	0.04	0.01	0.07	0.04	0.05	0.07	0.06	0.06	0.09	0.34	0.03	0.11

**Notes.** <sup>†</sup>: GSC02883-01687

**Table 3.** Carbon and oxygen abundances for the MS stars from MA15.

HIP	C I	O I
171	-0.52 ± 0.02	-0.25 ± 0.02
490	-0.14 ± 0.05	
522	0.04 ± 0.03	
544	0.00 ± 0.02	
1598	-0.30 ± 0.01	
1599	-0.26 ± 0.02	-0.09 ± 0.01
2941		0.15 ± 0.02
3093	0.09 ± 0.04	0.13 ± 0.02
3765	0.05 ± 0.20	-0.12 ± 0.03
3821	-0.20 ± 0.04	-0.15 ± 0.01
3909	-0.09 ± 0.04	
4148	0.36 ± 0.03	
5336		0.61 ± 0.02
5862	0.18 ± 0.02	
5944	0.06 ± 0.13	
7513	0.12 ± 0.02	
7576		
7978	-0.14 ± 0.01	
7981	-0.06 ± 0.04	0.12 ± 0.02
8486	-0.19 ± 0.01	
10138	-0.17 ± 0.03	0.07 ± 0.02
10798	-0.36 ± 0.02	-0.16 ± 0.02
12114	0.68 ± 0.03	
12777	-0.05 ± 0.02	
13402	0.05 ± 0.03	-0.02 ± 0.02
13642	0.29 ± 0.03	
14632	0.13 ± 0.01	-0.03 ± 0.01
15330	-0.21 ± 0.04	
15371	-0.21 ± 0.06	-0.05 ± 0.01
15457	-0.05 ± 0.01	
16537	0.10 ± 0.04	-0.07 ± 0.03
17420	0.36 ± 0.03	-0.09 ± 0.03
19849	0.00 ± 0.06	-0.04 ± 0.02
19855	-0.17 ± 0.01	
22263	-0.10 ± 0.02	-0.11 ± 0.01
23311	1.00 ± 0.04	0.42 ± 0.03
23816	0.00 ± 0.02	-0.19 ± 0.02
24205	-0.22 ± 0.02	-0.27 ± 0.01
24786		-0.11 ± 0.02
24813	0.03 ± 0.03	0.09 ± 0.01
25110	0.04 ± 0.03	
26779	0.06 ± 0.03	0.36 ± 0.02
27072	-0.12 ± 0.01	
27913	-0.17 ± 0.14	
27980	-0.01 ± 0.03	-0.31 ± 0.01
28767	0.11 ± 0.07	
28954		
29271	0.03 ± 0.02	-0.24 ± 0.01
29568	-0.18 ± 0.01	
31711	-0.31 ± 0.01	
32439	-0.02 ± 0.04	
32480	0.02 ± 0.04	
32970	0.38 ± 0.09	-0.18 ± 0.02
32984	0.83 ± 0.03	
33212	-0.11 ± 0.03	
33277	-0.14 ± 0.13	
33690	0.11 ± 0.06	
33719	0.13 ± 0.02	-0.13 ± 0.02
34017	-0.02 ± 0.03	
34065	-0.09 ± 0.01	-0.02 ± 0.01

**Table 3.** Continued.

HIP	C I	O I
35136	$-0.23 \pm 0.04$	
36439	$-0.25 \pm 0.02$	
36827		
37853	$-0.43 \pm 0.06$	$-0.30 \pm 0.01$
38784	$-0.11 \pm 0.01$	
39903	$-0.50 \pm 0.06$	
40843	$-0.26 \pm 0.02$	
41484	$-0.02 \pm 0.01$	
41926	$-0.35 \pm 0.02$	$-0.32 \pm 0.02$
42074		
42333	$-0.01 \pm 0.01$	
42438	$-0.14 \pm 0.01$	
42808	$0.21 \pm 0.03$	
43625	$-0.26 \pm 0.14$	
43726	$0.05 \pm 0.01$	$0.18 \pm 0.01$
44897		$0.22 \pm 0.03$
45617		
46580		$-0.19 \pm 0.03$
47007	$0.19 \pm 0.01$	$0.20 \pm 0.02$
47592		
49081		$-0.02 \pm 0.01$
49699	$0.47 \pm 0.03$	
50384	$-0.32 \pm 0.01$	
51459	$-0.15 \pm 0.02$	
52462	$0.08 \pm 0.03$	
53721	$0.04 \pm 0.02$	$-0.03 \pm 0.01$
54745	$0.03 \pm 0.18$	
56452		$0.09 \pm 0.02$
56997	$-0.07 \pm 0.02$	
57507	$-0.20 \pm 0.02$	$-0.31 \pm 0.02$
58451	$0.27 \pm 0.11$	$-0.11 \pm 0.03$
60074	$-0.14 \pm 0.03$	
61028	$0.23 \pm 0.05$	
61100		
62145		$-0.20 \pm 0.03$
62207	$-0.51 \pm 0.07$	
62523		
63742		
64394	$-0.02 \pm 0.01$	$0.11 \pm 0.02$
64792	$0.08 \pm 0.12$	
64797	$0.16 \pm 0.03$	$-0.01 \pm 0.02$
65515		
65530		
66704	$-0.32 \pm 0.01$	
66781		
67275	$0.13 \pm 0.05$	
67422	$1.07 \pm 0.04$	$0.22 \pm 0.03$
67620	$-0.04 \pm 0.09$	$0.41 \pm 0.01$
68184	$0.90 \pm 0.03$	$0.41 \pm 0.03$
68593	$-0.02 \pm 0.03$	$0.26 \pm 0.03$
68682		
69965	$-0.59 \pm 0.02$	
70319	$-0.18 \pm 0.01$	
70857	$-0.14 \pm 0.02$	$1.11 \pm 0.02$
71181	$0.49 \pm 0.03$	
71395		
71683	$0.22 \pm 0.04$	$0.17 \pm 0.01$
71743		
72339	$0.79 \pm 0.74$	$-0.18 \pm 0.02$
72567	$-0.01 \pm 0.04$	
72848	$0.02 \pm 0.03$	$0.72 \pm 0.02$



**Table 3.** Continued.

HIP	C I	O I
73100	0.07 ± 0.04	
73869	-0.05 ± 0.01	
74702	-0.16 ± 0.12	
76375	0.31 ± 0.12	0.19 ± 0.03
76635	0.05 ± 0.04	0.29 ± 0.02
77052		
77372	0.06 ± 0.55	0.39 ± 0.02
77408		1.07 ± 0.02
77801	-0.23 ± 0.15	
78072	-0.39 ± 0.24	
78775		
79248		
79492	-0.16 ± 0.10	0.21 ± 0.02
79672	0.02 ± 0.02	0.06 ± 0.01
80337	-0.11 ± 0.07	
80725		
80902	-0.14 ± 0.08	
81300	0.00 ± 0.05	1.13 ± 0.02
81800	-0.06 ± 0.01	
82588		
82860	-0.11 ± 0.02	
83389	-0.10 ± 0.05	1.04 ± 0.02
84862	-0.03 ± 0.09	
85235	-0.41 ± 0.02	
86036	-0.02 ± 0.03	-0.05 ± 0.02
88601	0.05 ± 0.02	0.14 ± 0.02
88745	-0.41 ± 0.01	
88972	0.18 ± 0.06	0.15 ± 0.03
89042	0.02 ± 0.06	
91438	-0.23 ± 0.07	-0.08 ± 0.02
93017		
93858	0.05 ± 0.02	0.07 ± 0.01
94050	-0.03 ± 0.02	
94346		
95149	-0.08 ± 0.01	
96100	-0.27 ± 0.02	-0.05 ± 0.02
96901	0.03 ± 0.01	0.04 ± 0.01
97546	0.03 ± 0.02	
97675	0.07 ± 0.01	
98819		0.46 ± 0.02
99240	0.30 ± 0.07	-0.07 ± 0.01
99316		
99461	0.25 ± 0.07	-0.31 ± 0.03
99711		
101997		0.02 ± 0.02
103389	-0.19 ± 0.06	
104239	0.05 ± 0.03	
104903	0.13 ± 0.04	0.40 ± 0.01
105312	-0.20 ± 0.02	
105388	-0.17 ± 0.02	
105858	-0.49 ± 0.05	
106696	0.12 ± 0.03	
107022	0.04 ± 0.15	-0.08 ± 0.02
107350	-0.13 ± 0.02	
107649	-0.01 ± 0.14	
108028	0.24 ± 0.03	-0.24 ± 0.03
109422	0.00 ± 0.03	
109821	-0.06 ± 0.01	-0.09 ± 0.01
110109	-0.22 ± 0.06	-0.14 ± 0.01
114236	0.43 ± 0.02	
114622	0.59 ± 0.20	-0.09 ± 0.03

**Table 3.** Continued.

HIP	C I	O I
114948	$-0.09 \pm 0.02$	
115331		
116613		
116745	$1.35 \pm 0.39$	
116906	$-0.02 \pm 0.01$	$0.04 \pm 0.01$